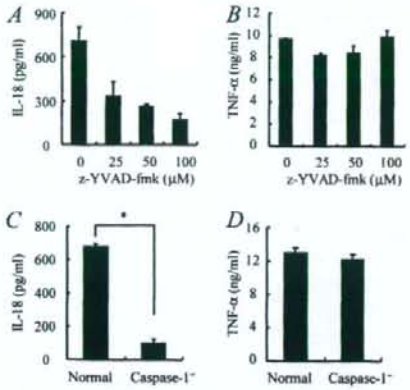

FIGURE 3. Caspase-1-dependent IL-18 production on LM infection. *A* and *B*, Adherent PECs were infected with wild-type LM. The cells were cultured for an additional 24 h in the presence of gentamicin with or without z-YVAD-fmk. *C* and *D*, Adherent PECs from normal and caspase-1 knockout mice were infected with wild-type LM. Cells were cultured for 24 h in the presence of gentamicin and then the culture supernatants were collected. The amounts of cytokines were determined by ELISA. Data represent the mean of triplicate assays and SD. Similar results were obtained in three independent experiments. *, $p < 0.01$.

next analyzed the levels of IL-18 mRNA in macrophages infected with each mutant strain. In contrast to the significant difference in the production of mature IL-18 shown above, there was no significant difference in the ability to induce the expression of IL-18 among all of the LM strains used (Fig. 2). Therefore the difference appeared to be dependent on the process that follows IL-18 gene expression.

Involvement of caspase-1 in the production of IL-18 induced by LM infection

Caspase-1, known also as IL-1β-converting enzyme, cleaves pro-IL-18 into mature form (20, 26–28). When macrophages were pre-treated with z-YVAD-fmk, a caspase-1-specific inhibitor, IL-18 production induced by wild-type LM was decreased in a dose-dependent manner (Fig. 3*A*). A nonspecific inhibitory effect of z-YVAD-fmk was ruled out, because the same concentration of this inhibitor did not affect the production of TNF-α (Fig. 3*B*). To further confirm the involvement of caspase-1 in LLO-dependent IL-18 maturation, macrophages from caspase-1-deficient mice were infected with wild-type LM and the levels of IL-18 in culture supernatants were then compared with those in macrophages from normal mice. As expected, there was a significant reduction of IL-18 production in caspase-1-deficient macrophages, whereas the same cells produced TNF-α at a level comparable to that produced by the cells from normal mice (Fig. 3, *C* and *D*).

Caspase-1 activation in macrophages infected with LM strains

On the basis of the above result, we have compared the expression and processing of caspase-1 between recombinant LM mutants producing either LLO or ILO. Quantitative real-time RT-PCR detection of caspase-1 mRNA in the peritoneal macrophages showed a constitutive expression even in the absence of infection, and there was no significant level of further induction by infection with any strain (Fig. 4*A*). Caspase-1 synthesized as an immature form is converted into active caspase-1 composed of p10 and p20 fragments by proteolytic cleavage and is released from the cells soon after the conversion (29, 30). To detect the active form of caspase-1 efficiently, we enriched caspase-1 in the culture supernatants by immunoprecipitation using anti-caspase-1 Ab, according to our own modification of the method reported recently (29). LLO-producing Δ*hly*::*hly* strongly induced the processing of immature caspase-1 as determined by the detection of a p10 fragment (Fig. 4*B*). A faint band could be observed also in lysate of macrophages infected with Δ*hly*::*ilo*; however, it never reached to the level observed by Δ*hly*::*hly* during 20 h of cultivation. Following the detection of the p10 fragment in the cell lysate, the activated form of caspase-1 became detectable only in the supernatant from the culture of macrophages infected with Δ*hly*::*hly* (Fig. 4*B*, *bottom*). The very faint level of p10 fragment induced by Δ*hly*::*ilo* infection never increased even if the culture time was extended to

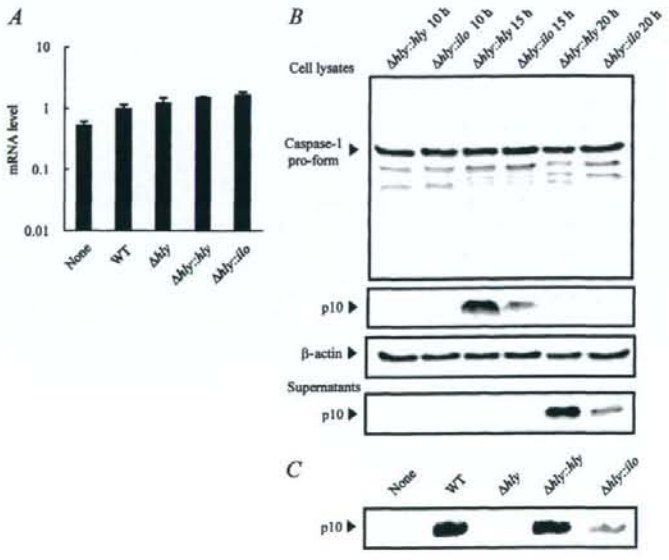

FIGURE 4. Expression and activation of caspase-1 in macrophages infected with LM strains. *A*, Adherent PECs were infected with each LM strain. The cells were cultured for an additional 5 h in the presence of gentamicin. Total RNA was extracted and subjected to quantitative real-time RT-PCR for detection of mRNA for caspase-1. Data represent the mean of triplicate assays and SD. *B*, The cells were cultured for an indicated time, and the culture supernatants were then collected. Adherent cells were lysed with 1% Nonidet P-40 lysis buffer. Active caspase-1 in the supernatants was immunoprecipitated and immunoblotted using a rabbit anti-caspase-1 Ab. *C*, After cultivation for 20 h, the active form of caspase-1 in the supernatants of the cells infected with each LM strain was detected. WT, Wild type.

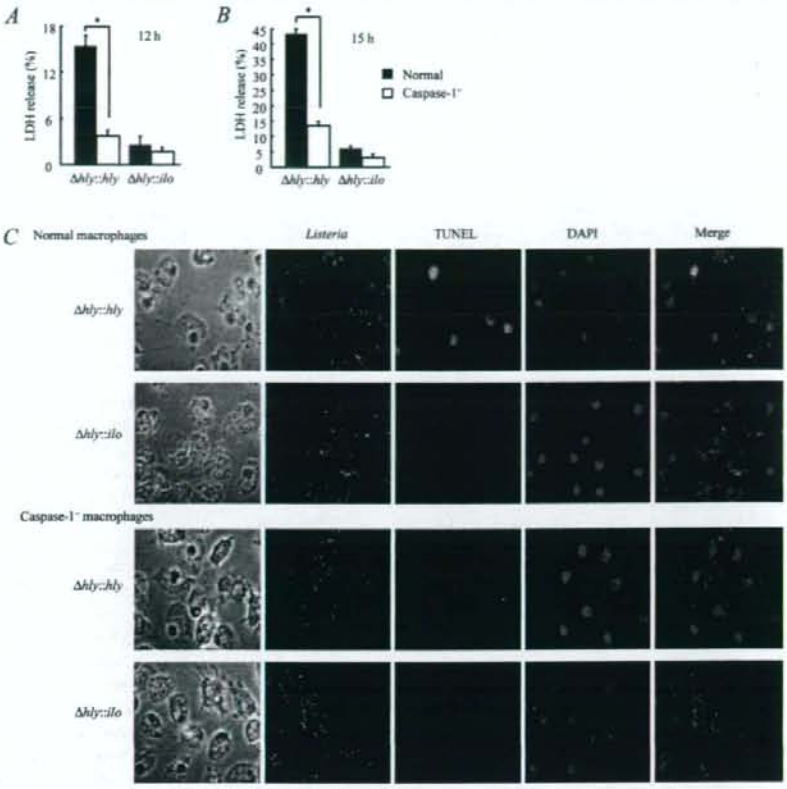

FIGURE 5. Detection of caspase-1-dependent cell death in macrophages infected with Δ*hly*::*hly* or Δ*hly*::*ilo*. *A* and *B*, Adherent PECs were infected with Δ*hly*::*hly* or Δ*hly*::*ilo*. The cells were cultured for an indicated time in the presence of gentamicin. The culture supernatants were collected and the LDH activity was assayed. Data represent the mean of triplicate assays and SD. Similar results were obtained in three independent experiments. *, $p < 0.01$. *C*, The cells were cultured for 21 h and visualized by staining for *Listeria* (red), fragmented DNA (green), and total nucleus (blue). DAPI, 4′,6-Diamidino-2-phenylindole.

30 h or of the MOI was increased to 10 (data not shown). The active form of caspase-1 was also detected in the supernatant from wild-type LM-infected macrophages, but not from Δ*hly*-infected cells (Fig. 4*C*). These results clearly indicated that caspase-1 activation induced upon infection with LM is dependent on not only the entry of bacteria into the macrophage cytoplasm but also the LLO molecule itself.

Caspase-1-dependent cell death of macrophages infected with LM strains

It has been reported that LM causes an unique type of cell death of the infected host macrophages, which is distinguished as pyroptosis from other forms of programmed cell death by its requirement of caspase-1 activation and the loss of plasma membrane integrity (21, 31). Other intracellular bacteria, *Salmonella* and *Shigella*, also induce pyroptosis accompanied by the release of LDH in a caspase-1-dependent manner only at an early phase of cell death, but not in late phases (32, 33). To know whether caspase-1-dependent events other than IL-18 maturation occur during infection with LLO-producing LM, we next determined LDH released from infected macrophages. The amount of LDH released from normal macrophages was higher than that from caspase-1-deficient macrophages when infection was done with Δ*hly*::*hly* (Fig. 5, *A* and *B*). In contrast, Δ*hly*::*ilo* induced a significantly lower level of LDH release compared with Δ*hly*::*hly*, and there was no significant difference in the amount of LDH released after infection with Δ*hly*::*ilo* between normal and caspase-1-deficient macrophages. Upon pyroptotic cell death, DNA cleavage occurred and could be detected by the TUNEL method (31, 34). Therefore we also tried to determine the level of pyroptosis by the visualization of fragmented DNA in *Listeria*-infected cells. As shown in Fig. 5*C* and Table I, TUNEL-positive cells were observed frequently in normal macrophages infected with Δ*hly*::*hly* but not in those infected with Δ*hly*::*ilo*. The DNA fragmentation induced by Δ*hly*::*hly* was caspase-1 dependent, because the number of TUNEL-positive cells was fewer and similar to the control level in the absence of caspase-1. These data indicated that LLO-producing LM, but not ILO-producing LM, induces a caspase-1-dependent pyroptosis in addition to the processing of IL-18 and supported our finding that the delivery of bacteria into the cytoplasm is not sufficient but that the presence of LLO is required for the induction of caspase-1 activation upon LM infection.

LLO-dependent caspase-1 activation does not require TLR4-mediated signaling

Because LLO has been reported as a ligand for TLR4 when added from outside of the cells (35), we examined the involvement of TLR4 in the production of IL-18 and the activation of caspase-1 in response to wild-type LM. Macrophages obtained from normal or TLR4-deficient mice were infected with LLO-producing wild-type LM and the culture supernatants were then subjected to cytokine assays. As shown in Fig. 6, *A–D*, the levels of cytokines, including IL-18, in supernatants of LM-infected TLR4-deficient macrophages were comparable to those of infected macrophages from normal mice, indicating that TLR4 is not involved in the production of IL-18 and other cytokines in response to the infection with LM. Furthermore, wild-type LM induced similar levels of caspase-1 activation in normal and TLR4-deficient macrophages

Table 1. *Percentage of TUNEL-positive (TUNEL$^+$) cells in Listeria-infected cells or total cells*

Macrophage	Bacteria	TUNEL$^+$/*Listeria*-Infected Cells (%) (Green/Red$^+$ Cell × 100)[a]	TUNEL$^+$/Total Cells (%) (Green/Blue × 100)[a]
Normal	None		1.95 ± 0.40
	Δ*hly*::*hly*	28.80 ± 1.83	15.83 ± 0.76
	Δ*hly*::*ilo*	4.60 ± 0.72	2.06 ± 0.20
Caspase-1$^-$	None		1.95 ± 0.20
	Δ*hly*::*hly*	5.73 ± 0.55	3.30 ± 0.36
	Δ*hly*::*ilo*	7.10 ± 1.41	3.06 ± 0.65

[a] Value represents means and SDs of three independent wells. Three hundred cells were examined in each well.

(Fig. 6*E*). From these results, it is indicated that the LLO-dependent caspase-1 activation and the subsequent production of mature IL-18 are not due to the recognition of LLO by TLR4.

Detection of the domain of LLO responsible for caspase-1 activation

To further confirm the involvement of LLO in caspase-1 activation induced upon LM infection, we constructed a Δ*hly*::*ilo* strain additionally expressing the full-length LLO by using the pAT28 expression vector. The activation of caspase-1 was observed when macrophages were infected with the Δ*hly*::*ilo* carrying full-length LLO expression vector, whereas Δ*hly*::*ilo* transformed with empty vector could not induce caspase-1 activation (Fig. 7*B*). Among the four domains comprising the whole LLO molecule, domain 4 is known as a cholesterol-binding domain and contains Trp-rich undecapeptide, which is highly conserved among cholesterol-dependent cytolysins and essential for the binding to membrane cholesterol (36). It has been previously reported that the domain 1–3 molecule of truncated LLO completely loses its cytolytic activity and the substitution of the third Trp of the undecapeptide (amino acid residue 492 of LLO holotoxin) with Ala severely attenuates the cytolytic activity of LLO (36, 37). Therefore, we next constructed Δ*hly*::*ilo* strains carrying each vector for the expression of LLO W492A or domain 1–3 of LLO to know whether cholesterol-binding and subsequent cytolysis by this cytolysin is required for the activation of caspase-1 in macrophages infected with LM. The production of different LLO molecules encoded by each plasmid was confirmed by Western blotting using an anti-LLO polyclonal Ab (Fig. 7*A*). The impaired ability of Δ*hly*::*ilo* in caspase-1 activation was restored by the introduction of a plasmid harboring the gene for full-length LLO, and such an effect was not affected even by the elimination of cytolytic activity as clearly shown by LLO W492A or LLO domain 1–3 (Fig. 7*B*). By contrast, complementation with a plasmid harboring the domain 4 of LLO, a molecule capable of cholesterol binding without cytolytic activity (38), never resulted in the acquisition of the ability for caspase-1 activation (Fig. 7*B*). As there was no significant difference in the level

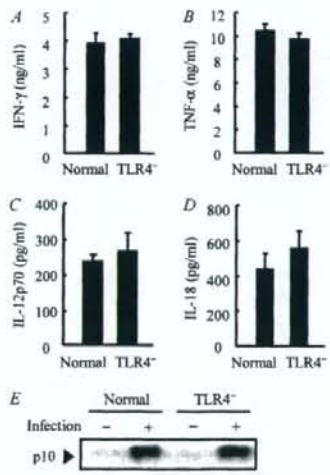

FIGURE 6. Cytokine production and caspase-1 activation in TLR4 knockout macrophages. *A–D*, Whole PECs (*A*) and adherent PECs (*B–D*) from normal and TLR4 knockout mice were infected with wild-type LM. Cells were cultured for 24 h in the presence of gentamicin and then the culture supernatant was collected. The amount of each cytokine was determined by using ELISA specific for each cytokine. Data represent the mean of triplicate assays and SD. Similar results were obtained in three independent experiments. *, $p < 0.01$. *E*, Adherent PECs from normal and TLR4 knockout mice were infected with wild-type LM. Cells were cultured for 20 h in the presence of gentamicin and the culture supernatants were collected. Active caspase-1 in the supernatants was immunoprecipitated and immunoblotted using a rabbit anti-caspase-1 Ab.

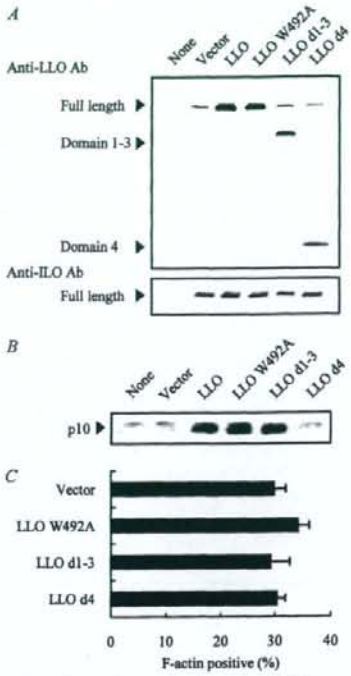

FIGURE 7. Detection of the domain (d) of LLO responsible for caspase-1 activation. *A*, Culture supernatants of Δ*hly*::*ilo* strains transformed with each LLO-expressing vector were applied to SDS-PAGE and subsequent Western blotting using anti-LLO Ab (*upper panel*) or anti-ILO Ab (*lower panel*). *B*, Adherent PECs were infected with each Δ*hly*::*ilo* strain, cultured for 20 h in the presence of gentamicin and spectinomycin (250 μg/ml), and culture supernatants were then collected. Active caspase-1 in the supernatants was immunoprecipitated and immunoblotted using a rabbit anti-caspase-1 Ab. *C*, Adherent PECs were infected with each Δ*hly*::*ilo* strain, cultured for 3 h in the presence of gentamicin and spectinomycin, and then bacteria and F-actin were stained and 300 bacteria were counted. The percentage of bacteria positive for associating F-actin was calculated for each strain. The filled bars represent the mean of three independent wells, and the error bars indicate the SD.

of F-actin-positive bacteria inside macrophages among these plasmid-carrying Δ*hly*::*ilo* strains (Fig. 7*C*), it was clearly indicated that domain 1–3 is the region responsible for the activation of caspase-1 in infected macrophages.

Discussion

We previously showed that an entry of bacteria into the cytoplasm was not sufficient for the IFN-γ response of mice to LLO-producing LM by both in vitro and in vivo experiments using two isogenic strains that differed only in LLO and ILO (11). In this study, we examined the difference between Δ*hly*::*hly* and Δ*hly*::*ilo* in the induction of IL-12 and IL-18, the two major IFN-γ-inducing cytokines, to elucidate the mechanism of LLO-dependent IFN-γ response to LM. It was noteworthy that LLO-producing LM, but not ILO-producing LM, strongly induced the production of IL-18. Because mRNA expression did not depend exclusively on LLO, we next examined the activation of caspase-1, which is essential for the maturation and secretion of biologically active IL-18. It was strongly suggested that the dependence of the IFN-γ response on LLO is due to the LLO-dependent induction of caspase-1 activation and subsequent IL-18 production and that the IL-18 response is dependent on not only the entry of bacteria into the macrophage cytoplasm but probably also on the distinct activity of LLO as a signaling ligand.

On the basis of a previous report (18) and our own similar observation (not shown) that IL-12 is not induced in mice deficient for MyD88, an adaptor molecule of almost all TLRs, upon infection with LM, it is clear that TLR-dependent recognition of bacterial ligands is essentially required for the induction of IL-12 production. By contrast, production of IL-18 is reported to be induced regardless of the absence of MyD88 (39). Our present finding that TLR4, a recognition receptor for LLO, was not involved in the activation of caspase-1 and production of IL-18 in macrophages infected with LM is consistent with these previous observations. Generally, IL-18 is constitutively expressed, and the produced pro-IL-18 remains inside the cells until being cleaved by activated caspase-1. Therefore both MyD88-dependent production of IL-12 and TLR4- and MyD88-independent cleavage of pro-IL-18 are likely the key processes for the induction of IFN-γ upon LM infection. Some distinct activity of LLO appeared to be involved in the latter process that cannot be induced by ILO.

Although the involvement of LLO in caspase-1-mediated IL-18 induction upon infection with LM was revealed clearly in this study, the mechanism remains to be elucidated. One possibility to be considered is the difference in the cytotoxic effect between LLO and ILO. These two cytolysins are highly homologous and exhibited a quite similar function regarding the contribution to the escape of *Listeria* from phagosome into the cytoplasm. After the escape of bacteria from the hazardous phagosome by means of cytolysin into the cytosol, a nutrient-rich niche for multiplication, it is important for the cytosolic bacteria to minimize further cytolytic activity to prevent host cell damage. For that, two mechanisms have been proposed: the dependency of cytolytic activity on acidic pH (40) and the presence of an N-terminal Pro-Glu-Ser-Thr (PEST)-like sequence, which is thought to target for phosphorylation and/or degradation in eukaryote cells (41). Although both LLO and ILO exhibited a similar optimal pH for cytolytic activity (42), the hemolytic activity of recombinant ILO was relatively higher than that of recombinant LLO (17). Besides, the sequence analysis of the *ilo* gene revealed the absence of the PEST-like sequence that is present in LLO (data not shown). In the present experimental results, the level of cytolysis induced by ILO-producing LM was marginal and rather lower than that induced by LLO-producing LM in caspase-1-deficient cells (Fig. 5). Moreover, these LM strains induced similar levels of TNF-α and IL-12 production by macrophages (Fig. 1). Therefore the above possibility could be ruled out, and the difference in the ability to induce IL-18 between LLO-producing LM and ILO-producing LM should be explained by other reasons. Construction of the Δ*hly* strains complemented with genes encoding chimeric proteins between LLO and ILO and recombinant strains expressing cytolysins mutated for PEST-like sequence, are under way, and the molecular basis for the LLO-dependent activation of caspase-1 should be clarified in the near future.

From our results using LLO-producing LM and ILO-producing LM, there may be two major possibilities as follows: 1) LLO activates some signaling pathway that leads to caspase-1 activation without the participation of any other ligands; and 2) LLO induces the activation of caspase-1 in cooperation with other bacterial ligands or merely enhances that induced by other bacterial ligands. If either of these possibilities is the case, ILO itself must have no or less ability to induce caspase-1 activation compared with LLO. In our previous study using recombinant LLO and ILO, it was shown that ILO is far less capable of inducing cytokines than LLO when added from outside of the cells in vitro (17). Therefore our assumption is that there is some molecular structure in LLO that is exclusively important for caspase-1 activation in the cytosol of macrophages. Indeed, our results using Δ*hly*::*ilo* strains additionally expressing the recombinant proteins of LLO molecule (Fig. 7) clearly indicated that domain 1–3 is the region responsible for such an activity after the escape of bacteria into the cytosolic space and also that the ability of the LLO molecule for membrane binding or membrane damage is not involved in the activation of caspase-1. In a further study, experiments on a transfection of macrophages with LLO- or ILO-expressing vector or an intracytosolic injection of recombinant cytolysin are to be conducted.

Compared with virulence gene expression in broth-cultured LM, the expression of LLO is believed to be up-regulated inside macrophages (43). It is therefore reasonable that some cytoplasmic sensor molecule, rather than a cell surface receptor, recognizes LLO, resulting in caspase-1 activation. It has been reported that LLO is recognized by TLR4 and activates a signaling pathway downstream of TLR4 (35). Moreover, recombinant LLO protein induced the production of various cytokines by splenocytes or PEC cultures in a TLR4-dependent manner, whereas recombinant ILO protein did not induce their production (17, 35). However, our present results indicated that TLR4 was not involved in the production of IL-18 and the activation of caspase-1 in macrophages infected with LM (Fig. 6). Several recent reports have shown that some bacterial ligands are recognized not only by TLRs but also by NLRs such as Ipaf/CARD12 and Nalp3/cryopyrin/Pypaf1, which are cytoplasmic proteins containing a leucine-rich repeat domain, a nucleotide-binding domain, and each signaling domain. Flagellin from *Salmonella* or *Legionella*, which is known as a TLR5 ligand (44), induces caspase-1 activation through an Ipaf-dependent pathway when it is in the cytoplasm (45–47). The small antiviral compounds imiquimod and R-848, which are TLR7 ligands (48), are also known to induce the activation of caspase-1 in a Nalp3-dependent manner (49). Moreover, Nalp1b, an NLR protein, is involved in the caspase-1-dependent cell death of mouse macrophages induced by lethal toxin, which is a protein toxin produced by *Bacillus anthracis*, suggesting that lethal toxin induces the activation of caspase-1 through Nalp1b directly or indirectly (50). In the case of infection with *Listeria*, caspase-1 activation in macrophages

is reported to depend upon an apoptosis-associated speck-like protein containing a C-terminal caspase recruitment domain, ASC, an adaptor molecule that links upstream NLRs to caspase-1 (20). Furthermore, it is reported that potassium efflux and the P2X7 receptor are not required for caspase-1 activation induced by *Listeria* infection (22). On the basis of these recent findings, it is highly possible that LM-induced caspase-1 activation is triggered by the recognition of cytosolic LLO by some NLR protein. The experiments in this line will be conducted also by using recombinant strains under construction.

In conclusion, this study has clearly indicated that LM-induced IFN-γ production in mice is ascribed mainly to the presence of LLO due to a distinct activity of inducing the activation of caspase-1 after evasion into the cytosolic space of infected macrophages.

Acknowledgments

We thank Keisuke Kuida (Vertex Pharmaceuticals) and Hiroko Tsutsui (Hyogo Medical University) for providing caspase-1 knockout mice.

Disclosures

The authors have no financial conflict of interest.

References

1. Schuchat, A., B. Swaminathan, and C. V. Broome. 1991. Epidemiology of human listeriosis. *Clin. Microbiol. Rev.* 4: 169–183.
2. Mocci, S., S. A. Dalrymple, R. Nishinakamura, and R. Murray. 1997. The cytokine stew and innate resistance to *L. monocytogenes*. *Immuno.l Rev.* 158: 107–114.
3. Cousens, L. P., and E. J. Wing. 2000. Innate defenses in the liver during *Listeria* infection. *Immunol. Rev.* 174: 150–159.
4. Edelson, B. T., and E. R. Unanue. 2000. Immunity to *Listeria* infection. *Curr. Opin. Immunol.* 12: 425–431.
5. Cossart, P., M. F. Vicente, J. Mengaud, F. Baquero, J. C. Perez-Diaz, and P. Berche. 1989. Listeriolysin O is essential for virulence of *Listeria monocytogenes*: direct evidence obtained by gene complementation. *Infect. Immun.* 57: 3629–3636.
6. Marquis, H., H. G. Bouwer, D. J. Hinrichs, and D. A. Portnoy. 1993. Intracytoplasmic growth and virulence of *Listeria monocytogenes* auxotrophic mutants. *Infect. Immun.* 61: 3756–3760.
7. Portnoy, D. A., P. S. Jacks, and D. J. Hinrichs. 1988. Role of hemolysin for the intracellular growth of *Listeria monocytogenes*. *J. Exp. Med.* 167: 1459–1471.
8. Thale, C., and A. F. Kiderlen. 2005. Sources of interferon-γ (IFN-γ) in early immune response to *Listeria monocytogenes*. *Immunobiology* 210: 673–683.
9. Plitas, G., U. I. Chaudhry, T. P. Kingham, J. R. Raab, and R. P. DeMatteo. 2007. NK dendritic cells are innate immune responders to *Listeria monocytogenes* infection. *J. Immunol.* 178: 4411–4416.
10. Yang, J., I. Kawamura, and M. Mitsuyama. 1997. Requirement of the initial production of γ interferon in the generation of protective immunity of mice against *Listeria monocytogenes*. *Infect. Immun.* 65: 72–77.
11. Hara, H., I. Kawamura, T. Nomura, T. Tominaga, K. Tsuchiya, and M. Mitsuyama. 2007. Cytolysin-dependent escape of the bacterium from the phagosome is required but not sufficient for induction of the Th1 immune response against *Listeria monocytogenes* infection: distinct role of listeriolysin O determined by cytolysin gene replacement. *Infect. Immun.* 75: 3791–3801.
12. Tanabe, Y., H. Xiong, T. Nomura, M. Arakawa, and M. Mitsuyama. 1999. Induction of protective T cells against *Listeria monocytogenes* in mice by immunization with a listeriolysin O-negative avirulent strain of bacteria and liposome-encapsulated listeriolysin O. *Infect. Immun.* 67: 568–575.
13. Xiong, H., Y. Tanabe, S. Ohya, and M. Mitsuyama. 1998. Administration of killed bacteria together with listeriolysin O induces protective immunity against *Listeria monocytogenes* in mice. *Immunology* 94: 14–21.
14. Kayal, S., and A. Charbit. 2006. Listeriolysin O: a key protein of *Listeria monocytogenes* with multiple functions. *FEMS Microbiol. Rev.* 30: 514–529.
15. Hof, H., and P. Hefner. 1988. Pathogenicity of *Listeria monocytogenes* in comparison to other *Listeria* species. *Infection* 16 (Suppl. 2): S141–S144.
16. Haas, A., M. Dumbsky, and J. Kreft. 1992. Listeriolysin genes: complete sequence of ilo from *Listeria ivanovii* and of lso from *Listeria seeligeri*. *Biochim. Biophys. Acta* 1130: 81–84.
17. Kimoto, T., I. Kawamura, C. Kohda, T. Nomura, K. Tsuchiya, Y. Ito, I. Watanabe, T. Kaku, E. Setianingrum, and M. Mitsuyama. 2003. Differences in γ interferon production induced by listeriolysin O and ivanolysin O result in different levels of protective immunity in mice infected with *Listeria monocytogenes* and *Listeria ivanovii*. *Infect. Immun.* 71: 2447–2454.
18. Seki, E., H. Tsutsui, N. M. Tsuji, N. Hayashi, K. Adachi, H. Nakano, S. Futatsugi-Yumikura, O. Takeuchi, K. Hoshino, S. Akira, et al. 2002. Critical roles of myeloid differentiation factor 88-dependent proinflammatory cytokine release in early phase clearance of *Listeria monocytogenes* in mice. *J. Immunol.* 169: 3863–3868.
19. Gu, Y., K. Kuida, H. Tsutsui, G. Ku, K. Hsiao, M. A. Fleming, N. Hayashi, K. Higashino, H. Okamura, K. Nakanishi, et al. 1997. Activation of interferon-γ inducing factor mediated by interleukin-1β converting enzyme. *Science* 275: 206–209.
20. Ozoren, N., J. Masumoto, L. Franchi, T. D. Kanneganti, M. Body-Malapel, I. Erturk, R. Jagirdar, L. Zhu, N. Inohara, J. Bertin, et al. 2006. Distinct roles of TLR2 and the adaptor ASC in IL-1β/IL-18 secretion in response to *Listeria monocytogenes*. *J. Immunol.* 176: 4337–4342.
21. Cervantes, J., T. Nagata, M. Uchijima, K. Shibata, and Y. Koide. 2007. Intracytosolic *Listeria monocytogenes* induces cell death through caspase-1 activation in murine macrophages. *Cell. Microbiol.* 10: 41–52.
22. Franchi, L., T. D. Kanneganti, G. R. Dubyak, and G. Nunez. 2007. Differential requirement of P2X7 receptor and intracellular K^+ for caspase-1 activation induced by intracellular and extracellular bacteria. *J. Biol. Chem.* 282: 18810–18818.
23. Ito, Y., I. Kawamura, C. Kohda, H. Baba, T. Nomura, T. Kimoto, I. Watanabe, and M. Mitsuyama. 2003. Seeligeriolysin O, a cholesterol-dependent cytolysin of *Listeria seeligeri*, induces γ interferon from spleen cells of mice. *Infect. Immun.* 71: 234–241.
24. Nomura, T., I. Kawamura, K. Tsuchiya, C. Kohda, H. Baba, Y. Ito, T. Kimoto, I. Watanabe, and M. Mitsuyama. 2002. Essential role of interleukin-12 (IL-12) and IL-18 for γ interferon production induced by listeriolysin O in mouse spleen cells. *Infect. Immun.* 70: 1049–1055.
25. Fukasawa, Y., I. Kawamura, R. Uchiyama, K. Yamamoto, T. Kaku, T. Tominaga, T. Nomura, S. Ichiyama, T. Ezaki, and M. Mitsuyama. 2005. Streptomycin-dependent exhibition of cytokine-inducing activity in streptomycin-dependent *Mycobacterium tuberculosis* strain 18b. *Infect. Immun.* 73: 7051–7055.
26. Mariathasan, S., D. S. Weiss, K. Newton, J. McBride, K. O'Rourke, M. Roose-Girma, W. P. Lee, Y. Weinrauch, D. M. Monack, and V. M. Dixit. 2006. Cryopyrin activates the inflammasome in response to toxins and ATP. *Nature* 440: 228–232.
27. Kanneganti, T. D., M. Body-Malapel, A. Amer, J. H. Park, J. Whitfield, L. Franchi, Z. F. Taraporewala, D. Miller, J. T. Patton, N. Inohara, and G. Nunez. 2006. Critical role for Cryopyrin/Nalp3 in activation of caspase-1 in response to viral infection and double-stranded RNA. *J. Biol. Chem.* 281: 36560–36568.
28. Tsuji, N. M., H. Tsutsui, E. Seki, K. Kuida, H. Okamura, K. Nakanishi, and R. A. Flavell. 2004. Roles of caspase-1 in *Listeria* infection in mice. *Int. Immunol.* 16: 335–343.
29. Pan, Q., J. Mathison, C. Fearns, V. V. Kravchenko, J. Da Silva Correia, H. M. Hoffman, K. S. Kobayashi, J. Bertin, E. P. Grant, A. J. Coyle, et al. 2007. MDP-induced interleukin-1β processing requires Nod2 and CIAS1/NALP3. *J. Leukocyte Biol.* 82: 177–183.
30. Qu, Y., L. Franchi, G. Nunez, and G. R. Dubyak. 2007. Nonclassical IL-1 β secretion stimulated by P2X7 receptors is dependent on inflammasome activation and correlated with exosome release in murine macrophages. *J. Immunol.* 179: 1913–1925.
31. Fink, S. L., and B. T. Cookson. 2006. Caspase-1-dependent pore formation during pyroptosis leads to osmotic lysis of infected host macrophages. *Cell. Microbiol.* 8: 1812–1825.
32. Mariathasan, S., K. Newton, D. M. Monack, D. Vucic, D. M. French, W. P. Lee, M. Roose-Girma, S. Erickson, and V. M. Dixit. 2004. Differential activation of the inflammasome by caspase-1 adaptors ASC and Ipaf. *Nature* 430: 213–218.
33. Suzuki, T., L. Franchi, C. Toma, H. Ashida, M. Ogawa, Y. Yoshikawa, H. Mimuro, N. Inohara, C. Sasakawa, and G. Nunez. 2007. Differential regulation of caspase-1 activation, pyroptosis, and autophagy via Ipaf and ASC in *Shigella*-infected macrophages. *PLoS Pathog.* 3: e111.
34. Bergsbaken, T., and B. T. Cookson. 2007. Macrophage activation redirects *Yersinia*-infected host cell death from apoptosis to caspase-1-dependent pyroptosis. *PLoS Pathog.* 3: e161.
35. Park, J. M., V. H. Ng, S. Maeda, R. F. Rest, and M. Karin. 2004. Anthrolysin O and other gram-positive cytolysins are Toll-like receptor 4 agonists. *J. Exp. Med.* 200: 1647–1655.
36. Michel, E., K. A. Reich, R. Favier, P. Berche, and P. Cossart. 1990. Attenuated mutants of the intracellular bacterium *Listeria monocytogenes* obtained by single amino acid substitutions in listeriolysin O. *Mol. Microbiol.* 4: 2167–2178.
37. Watanabe, I., T. Nomura, T. Tominaga, K. Yamamoto, C. Kohda, I. Kawamura, and M. Mitsuyama. 2006. Dependence of the lethal effect of pore-forming haemolysins of Gram-positive bacteria on cytolytic activity. *J. Med. Microbiol.* 55: 505–510.
38. Kohda, C., I. Kawamura, H. Baba, T. Nomura, Y. Ito, T. Kimoto, I. Watanabe, and M. Mitsuyama. 2002. Dissociated linkage of cytokine-inducing activity and cytotoxicity to different domains of listeriolysin O from *Listeria monocytogenes*. *Infect. Immun.* 70: 1334–1341.
39. Seki, E., H. Tsutsui, H. Nakano, N. Tsuji, K. Hoshino, O. Adachi, K. Adachi, S. Futatsugi, K. Kuida, O. Takeuchi, et al. 2001. Lipopolysaccharide-induced IL-18 secretion from murine Kupffer cells independently of myeloid differentiation factor 88 that is critically involved in induction of production of IL-12 and IL-1β. *J. Immunol.* 166: 2651–2657.
40. Glomski, I. J., M. M. Gedde, A. W. Tsang, J. A. Swanson, and D. A. Portnoy. 2002. The *Listeria monocytogenes* hemolysin has an acidic pH optimum to compartmentalize activity and prevent damage to infected host cells. *J. Cell Biol.* 156: 1029–1038.
41. Decatur, A. L., and D. A. Portnoy. 2000. A PEST-like sequence in listeriolysin O essential for *Listeria monocytogenes* pathogenicity. *Science* 290: 992–995.

42. Nomura, T., I. Kawamura, C. Kohda, H. Baba, Y. Ito, T. Kimoto, I. Watanabe, and M. Mitsuyama. 2007. Irreversible loss of membrane-binding activity of *Listeria*-derived cytolysins in nonacidic conditions: a distinct difference from allied cytolysins produced by other Gram-positive bacteria. *Microbiology* 153: 2250–2258.
43. Moors, M. A., B. Levitt, P. Youngman, and D. A. Portnoy. 1999. Expression of listeriolysin O and ActA by intracellular and extracellular *Listeria monocytogenes*. *Infect. Immun.* 67: 131–139.
44. Hayashi, F., K. D. Smith, A. Ozinsky, T. R. Hawn, E. C. Yi, D. R. Goodlett, J. K. Eng, S. Akira, D. M. Underhill, and A. Aderem. 2001. The innate immune response to bacterial flagellin is mediated by Toll-like receptor 5. *Nature* 410: 1099–1103.
45. Amer, A., L. Franchi, T. D. Kanneganti, M. Body-Malapel, N. Ozoren, G. Brady, S. Meshinchi, R. Jagirdar, A. Gewirtz, S. Akira, and G. Nunez. 2006. Regulation of *Legionella* phagosome maturation and infection through flagellin and host Ipaf. *J. Biol. Chem.* 281: 35217–35223.
46. Franchi, L., A. Amer, M. Body-Malapel, T. D. Kanneganti, N. Ozoren, R. Jagirdar, N. Inohara, P. Vandenabeele, J. Bertin, A. Coyle, et al. 2006. Cytosolic flagellin requires Ipaf for activation of caspase-1 and interleukin 1β in salmonella-infected macrophages. *Nat. Immunol.* 7: 576–582.
47. Miao, E. A., C. M. Alpuche-Aranda, M. Dors, A. E. Clark, M. W. Bader, S. I. Miller, and A. Aderem. 2006. Cytoplasmic flagellin activates caspase-1 and secretion of interleukin 1β via Ipaf. *Nat. Immunol.* 7: 569–575.
48. Hemmi, H., T. Kaisho, O. Takeuchi, S. Sato, H. Sanjo, K. Hoshino, T. Horiuchi, H. Tomizawa, K. Takeda, and S. Akira. 2002. Small anti-viral compounds activate immune cells via the TLR7 MyD88-dependent signaling pathway. *Nat. Immunol.* 3: 196–200.
49. Kanneganti, T. D., N. Ozoren, M. Body-Malapel, A. Amer, J. H. Park, L. Franchi, J. Whitfield, W. Barchet, M. Colonna, P. Vandenabeele, et al. 2006. Bacterial RNA and small antiviral compounds activate caspase-1 through cryopyrin/Nalp3. *Nature* 440: 233–236.
50. Boyden, E. D., and W. F. Dietrich. 2006. Nalp1b controls mouse macrophage susceptibility to anthrax lethal toxin. *Nat. Genet.* 38: 240–244.

Serodiagnosis of *Mycobacterium avium*–Complex Pulmonary Disease Using an Enzyme Immunoassay Kit

Seigo Kitada[1], Kazuo Kobayashi[2], Satoshi Ichiyama[3], Shunji Takakura[3], Mitsunori Sakatani[4], Katsuhiro Suzuki[4], Tetsuya Takashima[5], Takayuki Nagai[5], Ikunosuke Sakurabayashi[6], Masami Ito[7], Ryoji Maekura[1], for the MAC Serodiagnosis Study Group

[1]Department of Internal Medicine, National Hospital Organization (NHO) National Toneyama Hospital, Toyonaka-shi, Osaka, Japan; [2]Department of Immunology, National Institute of Infectious Diseases, Shinjuku-ku, Tokyo, Japan; [3]Department of Clinical Laboratory Medicine, Graduate School of Medicine, Kyoto University, Kyoto-shi, Kyoto, Japan; [4]Department of Internal Medicine, NHO Kinki-chuo Chest Medical Center, Sakai-shi, Osaka, Japan; [5]Department of Medicine, Osaka Prefectural Medical Center for Respiratory and Allergic Diseases, Habikino-shi, Osaka, Japan; [6]Department of Laboratory Medicine, Saitama Medical Center, Jichi Medical University, Saitama-shi, Saitama, Japan; and [7]Department of Internal Medicine, Sakamoto Hospital, Toyonaka-shi, Osaka, Japan

***Rationale*: The diagnosis of *Mycobacterium avium*–complex pulmonary disease (MAC-PD) and/or its discrimination from pulmonary tuberculosis (TB) is sometimes complicated and time consuming.**

***Objectives*: We investigated in a six-institution multicenter study whether a serologic test based on an enzyme immunoassay (EIA) kit was useful for diagnosing MAC-PD and for distinguishing it from other lung diseases.**

***Methods*: An EIA kit detecting serum IgA antibody to glycopeptidolipid core antigen specific for MAC was developed. Antibody levels were measured in sera from 70 patients with MAC-PD, 18 with MAC contamination, 37 with pulmonary TB, 45 with other lung diseases, and 76 healthy subjects.**

***Measurements and Main Results*: Significantly higher serum IgA antibody levels were detected in patients with MAC-PD than in the other groups ($P < 0.0001$). Setting the cutoff point at 0.7 U/ml resulted in a sensitivity and specificity of the kit for diagnosing MAC-PD of 84.3 and 100%, respectively. Significantly higher antibody levels were also found in patients with nodular-bronchiectatic disease compared with fibrocavitary disease in MAC-PD ($P < 0.05$). There was a positive correlation between the extent of disease on chest computed tomography scans and the levels of antibody ($r = 0.43$, $P < 0.05$) in patients with MAC-PD.**

***Conclusions:* The EIA kit is useful for the rapid diagnosis of MAC-PD and for differentiating MAC-PD from pulmonary TB and, if validated by studies in other populations, could find wide application in clinical practice.**

Keywords: nontuberculous mycobacteria; immunocompetence; sensitivity and specificity

AT A GLANCE COMMENTARY

Scientific Knowledge on the Subject

The diagnosis of pulmonary disease due to ubiquitous *Mycobacterium avium* complex (MAC) is complicated, and requires clinical findings together with repeatedly positive sputum culture.

What This Study Adds to the Field

An enzyme immunoassay kit for measuring human serum antibody to glycopeptidolipid core antigen specific for MAC was developed. The kit is useful for the serodiagnosis of MAC pulmonary disease and could find wide application in clinical practice.

The prevalence of disease due to nontuberculous mycobacteria has been increasing recently (1–5). In Japan, *Mycobacterium avium* complex (MAC) accounts for approximately 70% of nontuberculous mycobacterial disease (6). MAC is now widely recognized as an important pathogen that causes chronic and progressive pulmonary disease even in immunocompetent patients and not only in those who are immunosuppressed. The diagnosis of MAC-PD is complicated because, in contrast to *Mycobacterium tuberculosis*, MAC contamination of clinical specimens can come from environmental sources such as water, dust, and soil, and because this organism may colonize the respiratory tract without any accompanying invasive disease (4). Thus, isolation of MAC from sputa is often of no clinical significance. Diagnosis of pulmonary disease due to MAC is complicated and time consuming when made according to the guidelines of the American Thoracic Society (ATS) (1), because MAC is ubiquitous in nature and the diagnosis requires clinical findings and its repeated isolation from sputum. In addition, it is also difficult to discriminate MAC-PD from infection due to other mycobacteria in the absence of culture results, because clinical features, such as symptomatic or radiographic findings, are very similar in mycobacterial diseases. In the context of infection control, it is particularly important to distinguish between MAC-PD and pulmonary tuberculosis (TB).

To overcome these difficulties, we have developed a serologic test for the glycopeptidolipid (GPL) antigen specific for MAC, and have reported its clinical usefulness (7–9). The levels of antibody to GPL core were measured by an enzyme immunoassay (EIA) using sera of immunocompetent patients with MAC-PD. MAC-PD could be discriminated from pulmonary TB, *Mycobacterium kansasii* pulmonary disease and MAC colonization/contamination using this serologic test. Healthy subjects were seronegative. Of the different immunoglobulin (Ig) subclasses, best results were obtained by the measurement of IgA, with a sensitivity of 92.5% and specificity of 95.1%. These results suggest that the test is useful as a diagnostic aid. In the present study, to apply this test widely in clinical practice, we

(Received in original form May 25, 2007; accepted in final form December 13, 2007)

Supported by grants from the Ministry of Health, Labor, and Welfare (Research on Emerging and Re-emerging Infectious Diseases, Health Sciences research grants); the Ministry of Education, Culture, Sports, Science, and Technology; Tauns Laboratory, Inc.; and the Osaka Tuberculosis Research Foundation.

Correspondence and requests for reprints should be addressed to Seigo Kitada, M.D., Department of Internal Medicine, National Hospital Organization National Toneyama Hospital, 5-1-1 Toneyama, Toyonaka-shi, Osaka 560-8552, Japan. E-mail: kitadas@toneyama.hosp.go.jp

This article contains an online supplement, which is accessible from this issue's table of contents at www.atsjournals.org

Am J Respir Crit Care Med Vol 177. pp 793–797, 2008
Originally Published in Press as DOI: 10.1164/rccm.200705-771OC on December 13, 2007
Internet address: www.atsjournals.org

developed an EIA kit detecting serum IgA antibody specific for GPL core and investigated its usefulness in a multicenter study.

METHODS

See the online supplement for additional methodologic details.

Patients and Serum Samples

Six institutions participated in this study. Between June 2003 and December 2005, serum samples were collected from 70 patients with MAC-PD, 18 with MAC contamination, 36 with pulmonary TB, 45 with other lung diseases, and 76 healthy subjects. All patients with MAC-PD met the ATS guidelines (1). Of the 70 patients with MAC-PD, 64 had previously received combination chemotherapy for mycobacterial diseases recommended by the ATS guidelines, but had MAC-positive cultures at the time of serum collection. Pulmonary TB was confirmed by culture positivity for *M. tuberculosis*. Patients with pulmonary TB who had an underlying pulmonary disease or past history of treatment for pulmonary TB were excluded. Individuals with MAC contamination showed a single culture positive for MAC in small amounts, but were asymptomatic and had no significant chest computed tomography (CCT) findings indicating active mycobacterial disease. The other lung diseases included chronic obstructive pulmonary disease (n = 15), idiopathic interstitial pneumonia (n = 11), lung cancer (n = 11), bacterial pneumonia (n = 4), pulmonary sarcoidosis (n = 2), and bronchiectasis (n = 2). All sera were stored at −20°C until assayed for IgA GPL core antibody. None of the patients was seropositive for HIV type 1 or 2. The patients with MAC-PD were classified into two groups on the basis of the chest radiography: fibrocavitary disease and nodular-bronchiectatic (NBE) disease (1).

Fibrocavitary disease was defined as the presence of cavitary forms in upper lobes. NBE disease was defined as the presence of bronchiectasis and multiple nodular shadows on CCT. Disease conforming to neither of these types was considered unclassifiable. Forty-five patients underwent CCT and serodiagnosis at the same time. A correlation between the extent of disease and antibody levels was investigated. The extent of disease was expressed as the number of MAC-involved CCT segments, as described in the previous study (9).

The studies in human subjects were approved by the research and ethical committees of the NHO National Toneyama Hospital, and written, informed consent was obtained from all subjects.

EIA Kit

The EIA kit was developed by Tauns Laboratories, Inc. (Shizuoka, Japan), with a slight modification of the method described previously (8). Results are given as arbitrary U/ml in relation to a standard curve that was constructed by mixing sera from three patients with MAC-PD as a reference. The intra- and interplate coefficients of variation were 2.27–9.29% and 0.57–8.86%, respectively, which indicated good reproducibility. The linearity of measurement was confirmed. The influence of blood elements and temperature was examined, and revealed good stability. The assay was performed by a technologist with no prior knowledge of the clinical data.

Statistical Analysis

All statistical analyses were performed using GraphPad Prism version 4 (GraphPad Software, Inc., San Diego, CA). Antibody levels in patient groups are expressed as means ± SD. For comparison of the mean values of multiple groups, data were compared by analysis of variance and nonparametric analysis. A probability value of less than 0.05 was regarded as significant.

RESULTS

Study Subjects

The characteristics of the subjects are shown in Table 1. Patients with pulmonary TB and healthy subjects were younger than patients with MAC-PD ($P < 0.001$), and there was a larger proportion of females in the latter group ($P < 0.001$). Of the 70 patients with MAC-PD, 15 had underlying pulmonary disease, all of which were the sequelae of pulmonary TB. Of the 18 individuals with MAC contamination, 15 had underlying pulmonary diseases (8 patients with the sequelae of pulmonary TB, 2 with lung cancer, 2 with chronic obstructive pulmonary disease, 1 with emphysema, 1 with pneumoconiosis, and 1 with sarcoidosis. Of the patients with MAC-PD, 19 were classified as having fibrocavitary disease, and 35 as having NBE disease, with 16 patients unclassifiable. The MAC-PD group included infections with *M. avium* (n = 56), *Mycobacterium intracellulare* (n = 12), or both (n = 2). The MAC contamination group included *M. avium* (n = 16) and *M. intracellulare* (n = 2).

Level of GPL Core IgA Antibody

The level of serum IgA antibody to GPL core was quantified using the EIA kit (Figure 1). As expected, patients with MAC-PD had significantly higher levels than patients with MAC contamination, those with pulmonary TB, those with other lung diseases, and healthy subjects—namely, 10.7 ± 7.9, 0.2 ± 0.1, 0.1 ± 0.1, 0.0 ± 0.1, and 0.0 ± 0.0 U/ml, respectively ($P < 0.0001$). A receiver operating characteristic (ROC) curve was constructed for MAC-PD and the other groups to establish the best cutoff value (Figure 2). Setting the cutoff value at 0.7 U/ml resulted in 100% specificity, at a sensitivity of 84.3% (Table E1). Using the EIA kit allowed clear discrimination between patients with MAC-PD and MAC contamination, pulmonary TB, and other lung diseases, as well as healthy subjects.

Next, we compared levels of serum IgA antibody to GPL core in fibrocavitary disease and NBE disease of MAC-PD. Significantly higher levels were found in NBE ($P < 0.05$) (Figure 3). With the cutoff value set at 0.7 U/ml, positivity in NBE and fibrocavitary disease was 91.4 and 63.2%, respectively. In contrast, in patients with MAC-PD, no significant differences between *M. avium* and *M. intracellulare* as causative agents were observed ($P = 0.403$). The erythrocyte sedimentation rate in MAC-PD was 32.6 ± 28.6 mm/hour and there was a significant positive correlation between the erythrocyte sedimentation rate and antibody levels in patients with MAC-PD ($r = 0.294$, $P < 0.05$).

Radiographic Severity and the Level of GPL Core Antibody

Forty-five patients with MAC-PD (10 with fibrocavitary disease, 26 with NBE disease, and 9 with unclassifiable type disease) underwent CCT and serodiagnosis at the same time. Four patients with unclassifiable type disease were excluded from the investigation because it was hard to discriminate between MAC lesions and underlying pulmonary disease. There was a positive correlation between the extent of disease and the

TABLE 1. CHARACTERISTICS OF STUDY SUBJECTS

	MAC-PD	MAC Contamination	Pulmonary TB	Other Lung Disease	Healthy Subjects
Number	70	18	36	45	76
Age, mean yr ± SD	68.0 ± 9.6	64.6 ± 11.6	52.9 ± 16.6*	66.3 ± 10.9	38.1 ± 12.0*
Age range, yr	50–90	28–78	24–76	29–82	20–65
Sex, no. male/no. female	25/45	10/8	26/10*	34/11*	41/35*
Duration of disease, mean yr ± SD	4.8 ± 4.6		0.3 ± 0.2	2.2 ± 2.4	

* $P < 0.001$.

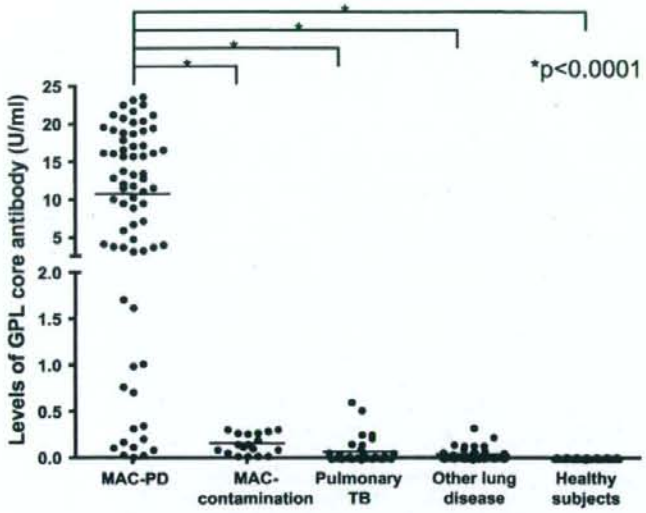

Figure 1. The level of serum IgA antibody to glycopeptidolipid (GPL) core antigen. Serum samples from six different institutions included 70 patients with *Mycobacterium avium* complex pulmonary disease (MAC-PD), 18 with MAC contamination, 37 with pulmonary tuberculosis (TB), 45 with other lung diseases, and 76 healthy subjects. Antibody levels in MAC-PD were significantly higher than in the other groups ($P < 0.0001$). All results are expressed as individual data, and *horizontal bars* indicate geometric means.

levels of the antibody ($r = 0.43$, $P < 0.05$) (Figure 4). The total numbers of involved segments were not different (7.8 ± 4.9 and 7.9 ± 4.2 in fibrocavitary and NBE disease, respectively). Of 26 patients with NBE disease, 9 had small thin wall cavities. A tendency toward elevated GPL core antibody levels was found in NBE patients with cavities compared with those without, but this trend was not statistically significant ($P = 0.08$).

DISCUSSION

We previously established a serologic test for MAC-PD using a mixture of GPLs and GPL core antigen, and reported the clinical application of the EIA method for quantifying antibody levels (7, 8). GPL is an antigen located on the surface of the MAC cell wall and determines the serotype. At present, 31 distinct serotype-specific GPLs have been identified, of which the complete structures of 14 have been identified (10–12). GPL consists of a core common to all MAC serotypes and a serotype-specific oligosaccharide. In the initial study to establish the serodiagnosis of MAC-PD, we used the whole GPL antigen, a mixture of 11 serotype-specific GPLs (7). We then found that the GPL core was the dominant antigenic epitope of GPL, and subsequently developed a serologic test using GPL core antigen (8). In the previous study, GPL core antibody (IgG, IgA, and IgM) levels were found to be elevated in sera of patients with MAC-PD, but not pulmonary TB, *M. kansasii*–PD, MAC colonization/contamination, and healthy subjects. The study showed that this serologic test was useful for diagnosing MAC-PD and for differentiating it from pulmonary TB and *M. kansasii*–PD. Consistent with this, Fujita and colleagues (13) reported elevated levels of antibody against the GPL core antigen in patients with MAC-PD but not in those with pulmonary TB. In our previous study (8), of the different Ig classes, best results were obtained by IgA, including an association with CCT findings. Thus, a higher level of serum IgA antibody to GPL core indicated a wider extent of MAC disease and larger nodule formation on CCT (9). Therefore, we have attempted to develop and to assess an EIA kit for quantifying serum IgA antibody to GPL core in the present study. Optical density levels were converted to U/ml using standard serum samples, which provided reliable and reproducible results. In this multicenter study, using the EIA kit, it was confirmed that patients with MAC-PD could be clearly differentiated from those with pulmonary TB, those with MAC contamination, those with other lung diseases, and healthy subjects. Similar to our previous studies (7–9), the sensitivity and specificity for diagnosing MAC-PD by the kit was high and the level of the antibody correlated with the extent of MAC-PD assessed using CCT.

Distinguishing pulmonary TB from MAC-PD in clinical practice using the EIA kit has proven useful. Differentiating TB from MAC is difficult because symptoms and radiographic findings are often similar among patients with pulmonary mycobacterial diseases. Patients with pulmonary TB require immediate treatment and isolation, whereas the diagnosis of MAC-PD does not necessitate rapidly starting antimicrobial therapy (1), and isolation is not required. GPL antigens, which are major cell surface antigens of MAC, are not present in the cell wall of *M. tuberculosis* complex (11). On the basis of this observation, patients with TB do not produce anti-GPL antibody. Indeed most patients with TB did not possess serum antibodies against GPLs (Figure 1) (7, 8). However, we cannot exclude the possibility that disease in patients with TB was of too short duration (MAC-PD, 4.8 ± 4.6 yr, vs. TB, 0.3 ± 0.2 yr) to have allowed immune responses and shed mycobacterial antigen. In this present study, with a cutoff level of 0.7 U/ml, all patients with TB were classified as seronegative. The levels of GPL core antibody in patients with pulmonary TB were very low or absent

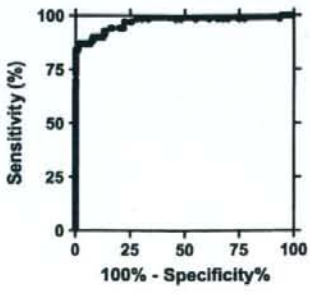

Figure 2. Receiver operating characteristic curve constructed for patients with *Mycobacterium avium*–complex pulmonary disease and the other groups.

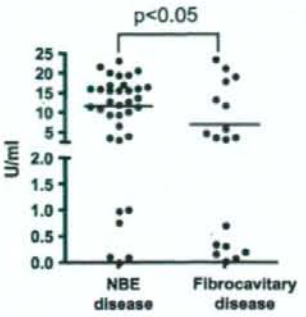

Figure 3. Levels of IgA antibody to glycopeptidolipid core antigens in nodular-bronchiectatic (NBE) and fibrocavitary subtypes of patients with *Mycobacterium avium* complex pulmonary disease (MAC-PD). Significantly higher levels were found in patients with MAC-PD with NBE compared with fibrocavitary disease ($P < 0.05$).

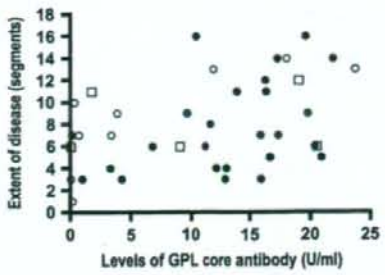

Figure 4. Correlation between antibody levels and radiographic severity using chest computed tomography in 41 patients with *Mycobacterium avium*–complex pulmonary disease. There was a positive correlation between the extent of disease and the levels of antibody ($r = 0.43$, $P < 0.05$). *Closed circles* represent patients with nodular-bronchiectatic disease, *open circles* represent patients with fibrocavitary disease, and *open squares* represent patients with unclassifiable type disease.

(0.1 ± 0.1 U/ml). In contrast, in previous studies (7, 8, 13), GPL seropositivity in patients with pulmonary TB ranged between 5.2 and 25%. One possible explanation for this previously reported lack of specificity may be that there was latent coinfection of MAC in patients with pulmonary TB. In the present study, however, we attempted to exclude patients with such latent coinfection because the entry criteria precluded patients having underlying lung disease or past history of pulmonary TB. Patients with lung diseases such as chronic obstructive pulmonary disease associated with smoking, bronchiectasis, previous mycobacterial disease, cystic fibrosis, and pneumoconiosis are prone to have MAC coinfection (1). In addition, future studies are needed to verify the cutoff value obtained from the ROC analysis using another sample of cases and controls on a much larger scale.

MAC-PD has recently been classified into two distinct subtypes: fibrocavitary disease and NBE disease (1). Fibrocavitary disease, the most common manifestation of MAC-PD, is usually seen in middle-aged or elderly men predisposed to lung disease due to smoking and alcohol drinking. This subtype of disease, generally progressive, is similar to pulmonary TB on chest radiography. If left untreated, it can lead to extensive lung destruction and death. In contrast, NBE disease is mostly seen in nonsmoking middle-aged or elderly women without predisposing lung disease. The clinical course is usually slower and less dramatic. Patients with NBE are presumed to have had a long subclinical period before appearance of disease manifestations. Significantly higher levels of GPL core antibody were seen in NBE than in fibrocavitary disease ($P < 0.05$) and higher seropositivity was found in patients with the former (91.4% compared with 63.2%). There were no significant differences of extent of disease between the two groups in patients who underwent CCT and serodiagnosis at the same time. Therefore, the results suggested the possibility that the antibody levels tend not to elevate in patients with fibrocavitary disease. This may reduce the utility of serodiagnosis for discriminating cavitary MAC from cavitary TB. However, the antibody would probably be present at high levels in patients with extensive lesions in fibrocavitary disease as was indeed found in three patients (17.9 ± 5.9 U/ml) who had extensive lesions (more than 13 segments) (Figure 4). Further investigations are required for confirmation of this notion in a larger study.

Of the 70 patients with MAC-PD, 64 had previously received combination chemotherapy, as recommended by the ATS guidelines (1). However, all had MAC-positive cultures at the time of serum collection, and were considered to have active MAC-PD. Thus, antibody levels were not changed by the failure of chemotherapy—that is, there was no conversion to seronegative from seropositive status (8); therefore, effects of the previous treatment on antibody levels were limited. Obviously, it would nonetheless be better to enroll chemotherapy-naive patients from diverse ethnic and racial populations and different geographic areas in future studies.

At present, the diagnosis of MAC-PD is usually made according to the ATS guidelines, which include clinical, radiographic, and microbiological criteria (1). The latter requires multiple positive cultures for MAC from sputum, a positive culture from bronchial lavage or a lung biopsy specimen, together with the other diagnostic features. Although it is easy to meet the criteria in advanced-stage MAC-PD, it is often difficult in early-stage disease. In clinical routine, it is impractical to obtain multiple sputum samples or perform bronchoscopy to obtain bronchial washings or lung tissue in all patients. It is also time consuming, because a long duration is required before the results of multiple cultures are available. There are several rapid methods for identification of MAC, but they have some limitations. The liquid culture–based system using radiometry and fluorometry allows the detection of mycobacterial growth at an early stage, fewer than 7 days for nontuberculous mycobacteria. However, limitations of this system include the inability to observe colony morphology, difficulty in recognizing mixed cultures, overgrowth by contaminations, cost, and radioisotope disposal. Rapid identification of MAC is also possible using DNA hybridization, nucleic acid amplification, or high-pressure liquid chromatography (1). The use of molecular biological technology has shortened the time required to identify mycobacteria from several weeks to as little as 1 day. The overall sensitivity for detecting MAC varies between 70 and 100%, with a specificity greater than 98%. However, the inability to distinguish live and dead organisms precludes nucleic acid amplification for definite diagnosis of active disease (14).

The EIA kit is a rapid (within a few hours) and noninvasive assay with high sensitivity (84.3%) and specificity (100%) for diagnosing MAC-PD. Using the EIA kit, as reported here, MAC-PD could be efficiently differentiated from MAC contamination. "MAC contamination" defined in the present study was considered to represent contamination from the environment, because patients were asymptomatic and revealed no significant CCT findings indicating active mycobacterial disease. Most of those people classified into the MAC contamination group were so categorized based on a single positive MAC culture by chance during the follow-up period after completion of chemotherapy for pulmonary TB or at routine examination on admission for other diseases. It is difficult to be certain that MAC contamina-

tion, as defined here, does not indicate subclinical infection because no confirmatory pathology was obtained. However, if MAC contamination does reflect subclinical infection, it is of little clinical importance and does not mandate therapy.

There were 15.7% false-negative EIA determinations in patients with MAC-PD. In such cases, diagnosis of MAC-PD should be made according to the ATS guidelines, as previously described. There are several possible explanations for these false-negative results, including the following: (*1*) recently diagnosed disease; (*2*) change of GPL core antigenicity after chemotherapy; or (*3*) diversity of immune responses to GPL core in individual patients, potentially governed by HLA genes (15). Therefore, it might be expected that not all patients with MAC-PD are capable of producing antibody to GPL core. Although the specificity determined here for the EIA kit was high, there remains also the possibility of false-positive results in patients with disease due to other mycobacteria, such as *Mycobacterium fortuitum*, *Mycobacterium chelonae*, *Mycobacterium abscessus*, and *Mycobacterium scrofulaceum*, because these organisms also possess GPL on their cell wall surface (10, 11, 16). Indeed, we have detected seropositivity in several patients with culture-positive *M. fortuitum* (data not shown). The incidence of pulmonary disease due to these other mycobacteria is relatively low (<5%) in Japan and the United States (6, 17), but a report from South Korea documented a high incidence of pulmonary infection by *M. abscessus* or *M. fortuitum* (33 and 11%, respectively (18). Therefore, caution is necessary when interpreting the results of the EIA kit in locations where other mycobacterial infections are endemic.

A recent study using high-resolution CT documented that characteristic findings with multiple small nodular shadows combined with bronchiectasis are predictive for culture-positive MAC with a relatively high probability. Swenson and colleagues (19) reported that, of 15 patients with these characteristic findings, 8 (53%) had cultures positive for MAC. Tanaka and coworkers (20) reported that, of 26 similar patients, 13 (50%) had positive cultures for MAC in bronchial washings. Therefore, combining positive results obtained by the EIA and the characteristic findings of high-resolution CT should yield a definitive diagnosis of MAC-PD even in patients with sputum culture–negative results for MAC. This approach may be useful especially in elderly patients with complications, in whom bronchoscopy cannot be performed.

In summary, the EIA kit for detection of serum IgA antibody specific for GPL core antigen is useful for rapid and accurate serodiagnosis of MAC-PD. Taken together with clinical, radiographic, and microbiological criteria, the kit may be a valuable tool for the diagnosis of MAC-PD. Validation of the EIA kit in the diagnosis of MAC-PD requires a larger controlled study in diverse populations.

Conflict of Interest Statement: None of the authors has a financial relationship with a commercial entity that has an interest in the subject of this manuscript.

References

1. Griffith DE, Aksamit T, Brown-Elliott BA, Catanzaro A, Daley C, Gordin F, Holland SM, Horsburgh R, Huitt G, Iademarco MF, *et al.*; ATS Mycobacterial Diseases Subcommittee. An official ATS/IDSA statement: diagnosis, treatment, and prevention of nontuberculous mycobacterial diseases. *Am J Respir Crit Care Med* 2007;175:367–416.
2. Subcommittee of the Joint Tuberculosis Committee of the British Thoracic Society. Management of opportunist mycobacterial infections: Joint Tuberculosis Committee guidelines 1999. *Thorax* 2000;55:210–218.
3. Field SK, Fisher D, Cowie RL. *Mycobacterium avium* complex pulmonary disease in patients without HIV infection. *Chest* 2004;126:566–581.
4. Field SK, Cowie RL. Lung disease due to the more common nontuberculous mycobacteria. *Chest* 2006;129:1653–1672.
5. Khan K, Wang J, Marras TK. Nontuberculous mycobacterial sensitization in the United States: national trends over three decades. *Am J Respir Crit Care Med* 2007;176:306–313.
6. Sakatani M. Nontuberculous mycobacteriosis: the present status of epidemiology and clinical studies. *Kekkaku* 1999;74:377–384.
7. Kitada S, Maekura R, Toyoshima N, Fujiwara N, Yano I, Ogura T, Ito M, Kobayashi K. Serodiagnosis of pulmonary disease due to *Mycobacterium avium* complex with an enzyme immunoassay that uses a mixture of glycopeptidolipid antigens. *Clin Infect Dis* 2002;35:1328–1335.
8. Kitada S, Maekura R, Toyoshima N, Naka T, Fujiwara N, Kobayashi M, Yano I, Ito M, Kobayashi K. Use of glycopeptidolipid core antigen for serodiagnosis of *Mycobacterium avium* complex pulmonary disease in immunocompetent patients. *Clin Diagn Lab Immunol* 2005;12:44–51.
9. Kitada S, Nishiuchi Y, Hiraga T, Naka N, Hashimoto H, Yoshimura K, Miki K, Miki M, Motone M, Fujikawa T, *et al.* Serological test and chest computed tomography findings in patients with *Mycobacterium avium* complex lung disease. *Eur Respir J* 2007;29:1217–1223.
10. Aspinall GO, Chatterjee D, Brennan PJ. The variable surface glycolipids of mycobacteria: structures, synthesis of epitopes, and biological properties. *Adv Carbohydr Chem Biochem* 1995;51:169–242.
11. Brennan PJ, Nikaido H. The envelope of mycobacteria. *Annu Rev Biochem* 1995;64:29–63.
12. Fujiwara N, Nakata N, Maeda S, Naka T, Doe M, Yano I, Kobayashi K. Structural characterization of a specific glycopeptidolipid containing a novel N-acyl-deoxy sugar from mycobacterium intracellulare serotype 7 and genetic analysis of its glycosylation pathway. *J Bacteriol* 2007;189:1099–1108.
13. Fujita Y, Doi T, Maekura R, Ito M, Yano I. Differences in serological responses to specific glycopeptidolipid-core and common lipid antigens in patients with pulmonary disease due to *Mycobacterium tuberculosis* and *Mycobacterium avium* complex. *J Med Microbiol* 2006;55:189–199.
14. Hellyer TJ, Fletcher TW, Bates JH, Stead WW, Templeton GL, Cave MD, Eisenach KD. Strand displacement amplification and the polymerase chain reaction for monitoring response to treatment in patients with pulmonary tuberculosis. *J Infect Dis* 1996;173:934–941.
15. Arend SM, Geluk A, van Meijgaarden KE, van Dissel JT, Theisen M, Andersen P, Ottenhoff TH. Antigenic equivalence of human T-cell responses to mycobacterium tuberculosis-specific RD1-encoded protein antigens ESAT-6 and culture filtrate protein 10 and to mixtures of synthetic peptides. *Infect Immun* 2000;68:3314–3321.
16. Chatterjee D, Khoo KH. The surface glycopeptidolipids of mycobacteria: structures and biological properties. *Cell Mol Life Sci* 2001;58:2018–2042.
17. O'Brien RJ, Geiter LJ, Snider DE Jr. The epidemiology of nontuberculous mycobacterial diseases in the United States: results from a national survey. *Am Rev Respir Dis* 1987;135:1007–1014.
18. Koh WJ, Kwon OJ, Jeon K, Kim TS, Lee KS, Park YK, Bai GH. Clinical significance of nontuberculous mycobacteria isolated from respiratory specimens in Korea. *Chest* 2006;129:341–348.
19. Swensen SJ, Hartman TE, Williams DE. Computed tomographic diagnosis of *Mycobacterium avium-intracellulare* complex in patients with bronchiectasis. *Chest* 1994;105:49–52.
20. Tanaka E, Amitani R, Niimi A, Suzuki K, Murayama T, Kuze F. Yield of computed tomography and bronchoscopy for the diagnosis of *Mycobacterium avium* complex pulmonary disease. *Am J Respir Crit Care Med* 1997;155:2041–2046.

JOURNAL OF BACTERIOLOGY, Feb. 2008, p. 1064–1071 Vol. 190, No. 3
0021-9193/08/$08.00+0 doi:10.1128/JB.01370-07

Identification and Characterization of Two Novel Methyltransferase Genes That Determine the Serotype 12-Specific Structure of Glycopeptidolipids of *Mycobacterium intracellulare*[▽]

Noboru Nakata,[1]* Nagatoshi Fujiwara,[2] Takashi Naka,[3] Ikuya Yano,[3] Kazuo Kobayashi,[4] and Shinji Maeda[5]

Department of Microbiology, Leprosy Research Center, National Institute of Infectious Diseases, Tokyo, Japan[1]; Department of Host Defense, Osaka City University Graduate School of Medicine, Osaka, Japan[2]; Japan BCG Laboratory, Tokyo, Japan[3]; Department of Immunology, National Institute of Infectious Diseases, Tokyo, Japan[4]; and Molecular Epidemiology Division, Mycobacterium Reference Center, The Research Institute of Tuberculosis, Japan Anti-Tuberculosis Association, Tokyo, Japan[5]

Received 23 August 2007/Accepted 5 November 2007

The *Mycobacterium avium* complex is distributed ubiquitously in the environment. It is an important cause of pulmonary and extrapulmonary diseases in humans and animals. The species in this complex produce polar glycopeptidolipids (GPLs); of particular interest is their serotype-specific antigenicity. Several reports have described that GPL structure may play an important role in bacterial physiology and pathogenesis and in the host immune response. Recently, we determined the complete structure of the GPL derived from *Mycobacterium intracellulare* serotype 7 and characterized the serotype 7 GPL-specific gene cluster. The structure of serotype 7 GPL closely resembles that of serotype 12 GPL, except for O methylation. In the present study, we isolated and characterized the serotype 12-specific gene cluster involved in glycosylation of the GPL. Ten open reading frames (ORFs) and one pseudogene were observed in the cluster. The genetic organization of the serotype 12-specific gene cluster resembles that of the serotype 7-specific gene cluster, but two novel ORFs (*orfA* and *orfB*) encoding putative methyltransferases are present in the cluster. Functional analyses revealed that *orfA* and *orfB* encode methyltransferases that synthesize *O*-methyl groups at the C-4 position in the rhamnose residue next to the terminal hexose and at the C-3 position in the terminal hexose, respectively. Our results show that these two methyltransferase genes determine the structural difference of serotype 12-specific GPL from serotype 7-specific GPL.

The *Mycobacterium avium* complex (MAC) consists of two species, *M. avium* and *Mycobacterium intracellulare*, which are opportunistic pathogens of humans and animals. Human exposure to the MAC is common because organisms of this complex are ubiquitous in the environment: they have been isolated from water, soil, plants, house dust, and other sources. In fact, the MAC is the most common cause of disease attributable to nontuberculous mycobacteria in humans (9). The majority of MAC infections are acquired environmentally, and person-to-person transmission is considered to be rare. The treatment of MAC infection is difficult because the organisms are often resistant to standard antituberculosis drugs.

Many antigenic or immunoregulatory glycolipids with structural diversity are expressed on the mycobacterial cell wall. These molecules are considered to be involved in bacterial virulence through host immune responses (5, 14, 22, 23). It is necessary to elucidate the molecular structure, biochemical characteristics, and biological functions of the lipid components to better understand the mechanisms of pathogenesis and drug resistance of the MAC. The most prominent feature of the MAC is the presence of antigenic glycolipids, the glycopeptidolipids (GPLs), which are present on the cell surface (1). The standard method for differentiation of MAC strains is serologic typing based on the oligosaccharide (OSE) residue of the GPL. GPLs contain a tetrapeptide-amino alcohol core, D-phenylalanine-D-*allo*-threonine-D-alanine-L-alaninol (D-Phe-D-*allo*-Thr-D-Ala-L-alaninol), with an amido-linked 3-hydroxy or 3-methoxy C_{26}-to-C_{34} fatty acid at the N terminus of D-Phe (4). The D-*allo*-Thr and terminal L-alaninol are further linked with 6-deoxy-talose (6-d-Tal) and 3,4-di-*O*-methyl-rhamnose (3,4-di-*O*-Me-Rha), respectively. This core GPL is present in all species of the MAC and shows a common antigenicity (1). In the serotype-specific GPLs, a haptenic OSE is linked with the 6-d-Tal residue. To date, 31 distinct serotype-specific polar GPLs have been identified biochemically; the complete structures of GPLs are partly defined for serotype 1 to 4, 7, 8, 9, 12, 14, 17, 19 to 21, 25, and 26 GPLs (7, 10). On the other hand, it has been reported that serotype-specific GPLs participate in pathogenesis and immunomodulation in the host (2, 13). Modification of the GPL structure might play an important role not only in antigenicity but also in host immune responses and bacterial physiology (18). Recently, chemical synthesis of various haptenic OSEs was demonstrated, and the genes encoding glycosylation pathway enzymes for the biosynthesis of GPLs were identified and characterized (8, 12, 19, 21). However, genes responsible for serotype-specific glycosylation have yet to be analyzed for most of the serotypes.

* Corresponding author. Mailing address: Department of Microbiology, Leprosy Research Center, National Institute of Infectious Diseases, 4-2-1 Aoba-cho, Higashimurayama, Tokyo 189-0002, Japan. Phone: 81 (42) 391 8211. Fax: 81 (42) 394 9092. E-mail: n-nakata@nih.go.jp.

▽ Published ahead of print on 16 November 2007.

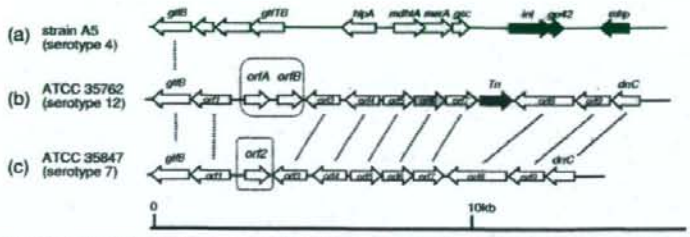

FIG. 2. Comparison of genetic organization of GPL biosynthesis clusters. (a) *M. avium* strain A5 organization, based on the annotated sequence obtained from GenBank (accession no. AY130970). (b) *M. intracellulare* ATCC 35762 (NF 103), sequenced in this study. (c) *M. intracellulare* ATCC 35847 (NF 027), sequenced in our previous study (GenBank accession no. AB274811). The orientation of each gene is shown by the arrow direction. The black arrows represent mobile elements, and the gray arrow represents a pseudogene. Mutually homologous ORFs and sequences are indicated with dotted lines.

elongated from D-*allo*-Thr was released as described previously (10, 15). Briefly, GPL was treated with 5 mg/ml sodium borohydride or borodeuteride in 0.5 N sodium hydroxide-ethanol (1:1 [vol/vol]) at 60°C for 16 h, with stirring. The reaction mixture was decationized with Dowex 50W X8 beads (The Dow Chemical Company, Midland, MI). The supernatant was collected and evaporated under nitrogen to remove boric acid. The dried residue was partitioned into two layers, using chloroform-methanol (2:1 [vol/vol]) and water. The upper aqueous phase was recovered and evaporated. In these processes, the OSE was purified as an oligoglycosyl alditol.

MALDI-TOF MS and MALDI-TOF/TOF MS analyses. The molecular species of the intact GPLs were detected using matrix-assisted laser desorption ionization–time-of-flight mass spectrometry (MALDI-TOF MS) with an Ultraflex II spectrophotometer (Bruker Daltonics, Billerica, MA). Each GPL was dissolved in chloroform-methanol (2:1 [vol/vol]) at a concentration of 1 mg/ml; 1 μl of a sample was then applied directly to the sample plate, followed by the addition of 1 μl of 10-mg/ml 2,5-dihydroxybenzoic acid in chloroform-methanol (1:1 [vol/vol]) as a matrix. The intact GPL was analyzed in the reflectron mode, with an accelerating voltage operating in positive mode at 20 kV (3). The OSE was analyzed by the fragment pattern with MALDI-TOF/TOF MS to determine the glycosyl composition. The OSE was dissolved with ethanol-water (3:7 [vol/vol]); the matrix was 10 mg/ml 2,5-dihydroxybenzoic acid in ethanol-water (3:7 [vol/vol]). The OSE and matrix were added to the sample plate by the same method as that for intact GPL. They were then analyzed in the lift-lift mode.

GC-MS analyses of alditol acetate derivatives. Gas chromatography (GC) and GC-MS analyses of partially methylated alditol acetate derivatives were performed to determine glycosyl compositions and linkage positions. Perdeuteromethylation was conducted using a modified procedure of Hakomori, as described previously (10, 11). Briefly, the dried OSE was dissolved with a mixture of dimethyl sulfoxide and sodium hydroxide, and deuteromethyl iodide was added. The reaction mixture was stirred at room temperature for 15 min, followed by the addition of water and chloroform. After centrifugation at 2,400 × *g* for 15 min, the upper water layer was discarded. The chloroform layer was washed twice with water and evaporated completely. To prepare partially deuteromethylated alditol acetates, perdeuteromethylated OSE was hydrolyzed using 2 N trifluoroacetic acid at 120°C for 2 h, reduced with 10 mg/ml sodium borodeuteride at 25°C for 2 h, and acetylated with acetic anhydride at 100°C for 1 h (6, 10, 16). GC-MS was then performed using a benchtop ion-trap mass spectrometer (Trace DSQ GC/MS; Thermo Electron Corporation, Austin, TX) equipped with a fused capillary column (30 m; 0.25-mm internal diameter) (Equity-1 or SP-2380; Supelco, Bellefonte, PA). Helium was used as the carrier gas, and the flow rate was 1 ml/min. The SP-2380 column was used for the analysis of alditol acetate derivatives. The temperature program was started at 60°C, with an increase of 40°C/min to 260°C and a hold at 260°C for 25 min. The Equity-1 column was used for analysis of perdeuteromethylated alditol acetate derivatives. The temperature program was 80°C for 1 min, with an increase of 20°C/min to 180°C followed by an increase of 8°C/min to 280°C.

Nucleotide sequence accession number. The nucleotide sequence reported here has been deposited in the NCBI GenBank database under accession number AB353739.

RESULTS

Cloning and sequence of the serotype 12 GPL biosynthesis cluster. To isolate the serotype 12-specific GPL biosynthesis gene cluster, a genomic cosmid library of an *M. intracellulare* serotype 12 strain, NF 103, was constructed. DNA was extracted from each clone by boiling. Using colony PCR with *rfbA* primers, the positive clone 161 was isolated from the *E. coli* transductants. Sequencing analysis revealed that cosmid clone 161 carried the DNA region from *gtfB* to *drrC*. Ten ORFs and one pseudogene other than *gtfB* and *drrC* were observed in the cluster (Table 1 and Fig. 2). The genetic organization between the *gtfB* and *drrC* genes (15.6 kb) of *M. intracellulare* NF 103 (serotype 12) closely resembled that of

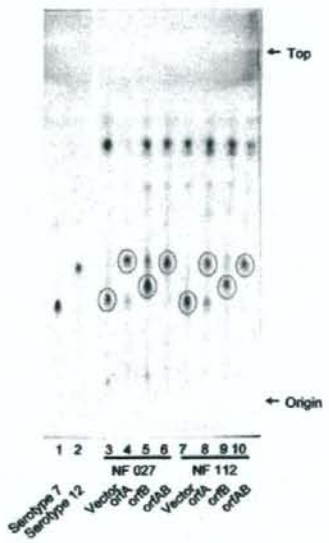

FIG. 3. TLC patterns of alkaline-stable lipids derived from *M. intracellulare* serotype 7 transformants. GPL 7 and GPL 12 were purified from *M. intracellulare* serotype 7 strain ATCC 35847 (NF 027) and serotype 12 strain ATCC 35762 (NF103). TLC was developed with a solvent system of chloroform-methanol-water (65:25:4 [vol/vol/vol]). Circled spots indicate prominent GPLs.

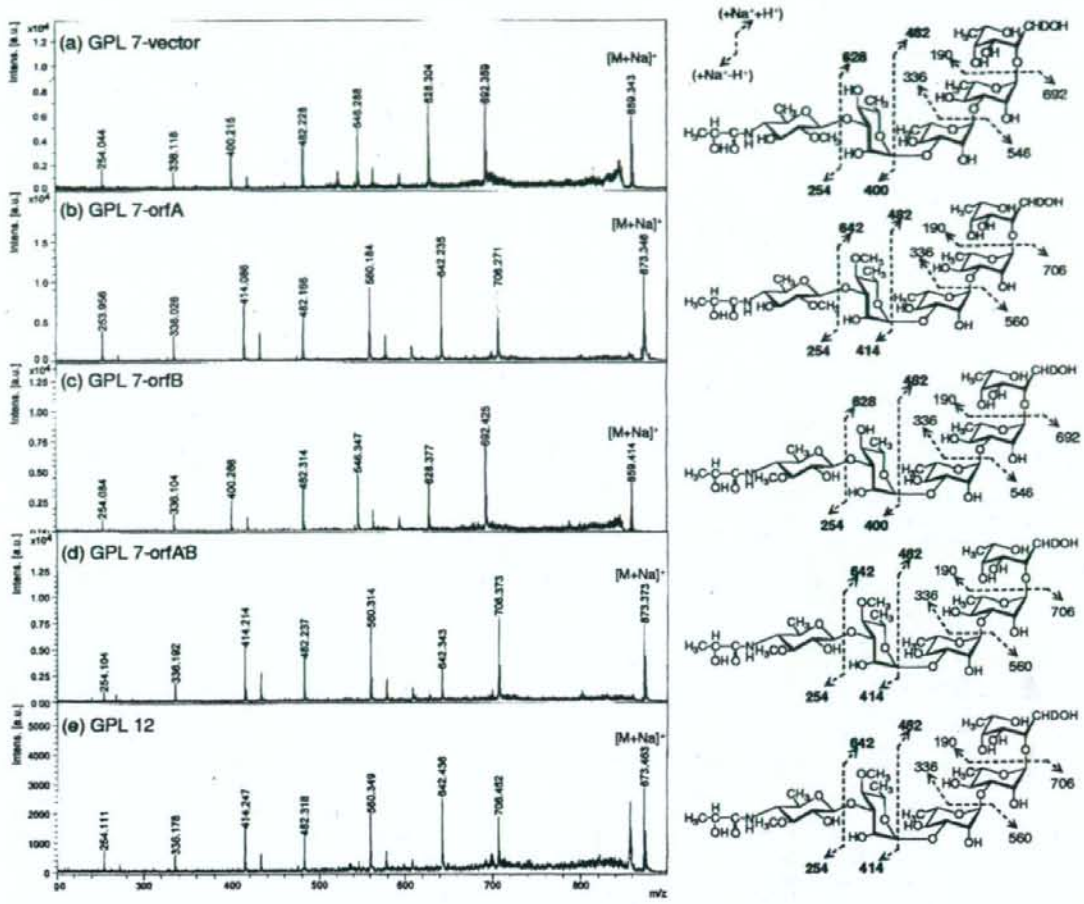

FIG. 5. Fragment patterns of MALDI-TOF/TOF MS spectra of OSEs in GPLs derived from *M. intracellulare* serotype 7, serotype 12, and serotype 7 transformants. The MALDI-TOF/TOF MS spectra were acquired using 10 mg/ml 2,5-dihydroxybenzoic acid in ethanol-water (3:7 [vol/vol]) as the matrix; the molecularly related ions were detected as $[M + Na]^+$ in lift-lift mode. The assigned fragment patterns of glycosyl residues are depicted. a.u., absorbance units.

mants were assigned as listed in Table 2. Altogether, the functions of the two genes were defined. The *orfA* product transfers a methyl group to the C-4 position of Rha next to the terminal sugar, and the *orfB* product transfers a methyl group to the C-3 position of the terminal sugar (Fig. 7). The results demonstrated that GPL 7 in the serotype 7 strain was changed completely to GPL 12 by introduction of the *orfA-orfB* gene cluster.

DISCUSSION

Nontuberculous mycobacteria, including the pathogenic species belonging to the MAC, have serotype-specific GPLs that are important components of the outer layer of the lipid-rich cell walls (5). Structural analyses of some serotype-specific GPLs derived from predominant clinical isolates have been reported (20). We recently determined the complete structure of serotype 7 GPL and the nucleotide sequence of the serotype 7-specific GPL biosynthesis cluster (10). In this cluster, Orfs 1, 3, and 9 might engender transfer of the two molecules of L-Rha and the terminal Hex of serotype 7 GPL (10). Orfs 4, 5, 7, and 8 are homologous to an aminotransferase, a carbamoyl phosphate synthase protein, a metallophosphoesterase, and an acyltransferase, respectively, and possibly relate to the biosynthesis of 2′-hydroxypropanoylamido in the terminal Hex. Based on analysis of sequence homology, these ORFs are probably responsible for the glycosylation of serotype 7 GPL. Serotype 12 GPL has a similar structure to that of serotype 7 GPL, except for O methylation (Fig. 1). In the present study, we cloned the serotype 12 GPL biosynthesis cluster and analyzed its sequence. Although the genetic organization of the *gtfB*-to-*drrC*

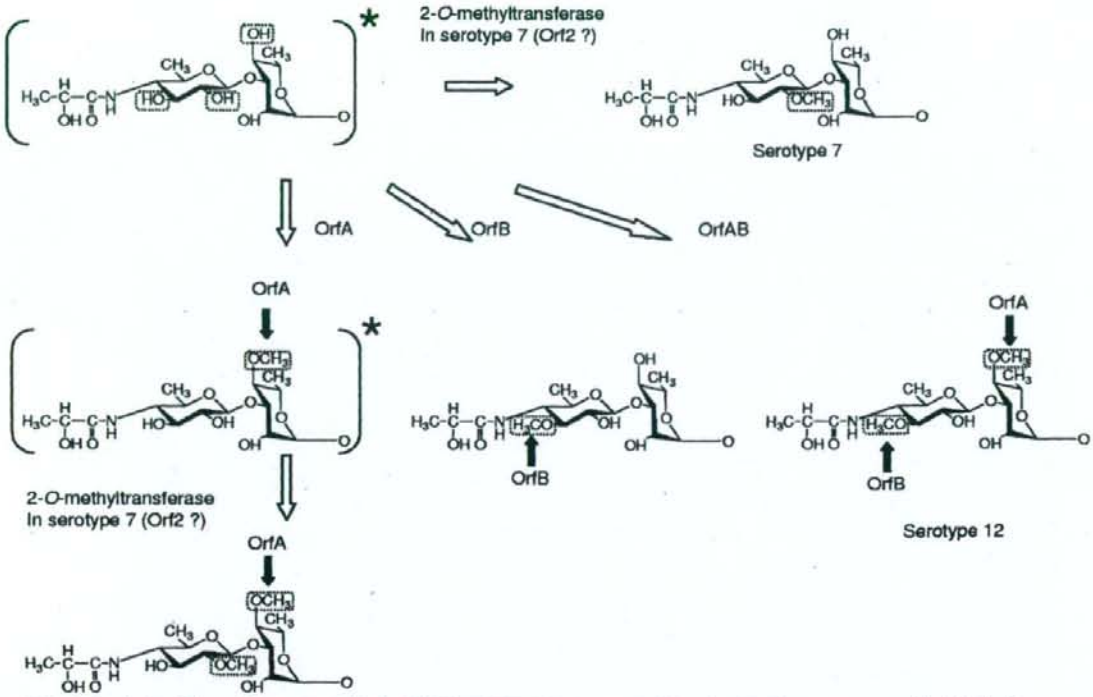

FIG. 7. Synthesis of *O*-methyl groups specific for GPL 7 and GPL 12 in the terminal disaccharide. The structures asterisked in the figure were not detected in this study. Serotype 12-specific O methylations and ORFs responsible for their syntheses are indicated by black arrows.

indicating that these two ORFs were responsible for producing the serotype 12-specific structure. The TLC patterns showed that the migration of GPL 7-orfB was different from that of GPL 7, although the MS data showed that they had the same molecular weight and the same number of methyl groups. A possible explanation for this is that a difference in the position of O methylation could influence hydrogen bond formation and the polarity of the whole molecule and consequently result in a different TLC migration pattern. GPL 7-orfB had an *O*-methyl group at C-3 but not at C-2 in the terminal Hex, indicating that the reaction of O methylation at C-2 by the 2-*O*-methyltransferase in serotype 7 is strongly inhibited by *O*-methylation at C-3. In addition, NF 027 transformed with *orfA* produced a trace of serotype 7-specifc GPL (Fig. 3, lane 4), and NF 027 transformed with *orfA* and *orfB* produced only serotype 12 GPL (Fig. 3, lane 6), suggesting that O methylation at C-2 in the terminal Hex might hinder the reaction of O methylation at C-4 in Rha next to the terminal Hex or that O methylation at C-3 in the terminal Hex might promote the reaction of O methylation at C-4 in Rha.

Because it is not likely that *M. intracellulare* serotypes 7 and 12 independently acquired different methyltransferase genes in the same genetic location between *orf1* and *orf3*, the common ancestor for these two serotypes possibly had all three genes and activated them as the occasion demanded. However, our results showed that reactions of O methylation at C-3 and C-2 in the terminal Hex were competitive (Fig. 3, lane 5, and Table 2). Tsang et al. (26) reported that the frequency of isolation of MAC organisms from AIDS or non-AIDS patients varied among serotypes and that *M. intracellulare* serotype 12 was isolated more often than serotype 7. These two serotypes of *M. intracellulare* might have evolved to adapt to certain environments by losing *orf2* or *orfA-orfB*.

Actually, GPLs are among the immunogenic molecules of the MAC. Tassel et al. reported that the core GPL seems to play a role in suppression of a mitogen-induced blastogenic response of spleen cells (25); furthermore, our previous study showed that sera of patients with MAC disease contain antibodies against GPLs and that the antibody level reflects disease activity (17). In addition, the immunomodulating activity of GPLs on macrophage functions is serotype dependent (13, 24). Elucidation of the structure-activity relationship of GPLs is necessary to better understand the pathogenesis of MAC infection.

ACKNOWLEDGMENTS

This work was supported by grants from the Ministry of Health, Labor and Welfare (Emerging and Re-Emerging Infectious Diseases), the Ministry of Education, Culture, Sports, Science and Technology of Japan, and the Japan Health Sciences Foundation.

N.N. is grateful to M. Kai and M. Makino for helpful discussions.

JOURNAL OF BACTERIOLOGY, May 2008, p. 3613–3621 Vol. 190, No. 10
0021-9193/08/$08.00+0 doi:10.1128/JB.01850-07

Structural Analysis and Biosynthesis Gene Cluster of an Antigenic Glycopeptidolipid from *Mycobacterium intracellulare*▽†

Nagatoshi Fujiwara,[1]* Noboru Nakata,[2] Takashi Naka,[1,3] Ikuya Yano,[3] Matsumi Doe,[4] Delphi Chatterjee,[5] Michael McNeil,[5] Patrick J. Brennan,[5] Kazuo Kobayashi,[6] Masahiko Makino,[2] Sohkichi Matsumoto,[1] Hisashi Ogura,[7] and Shinji Maeda[8]

Department of Host Defense[1] and Virology,[7] Osaka City University Graduate School of Medicine, Osaka 545-8585, Japan; Department of Microbiology, Leprosy Research Center, National Institute of Infectious Diseases, Tokyo 189-0002, Japan[2]; Japan BCG Laboratory, Tokyo 204-0022, Japan[3]; Department of Chemistry, Graduate School of Science, Osaka City University, Osaka 558-8585, Japan[4]; Department of Microbiology, Immunology and Pathology, Colorado State University, Colorado 80523[5]; Department of Immunology, National Institute of Infectious Diseases, Tokyo 162-8640, Japan[6]; and Molecular Epidemiology Division, Mycobacterium Reference Center, The Research Institute of Tuberculosis, Japan Anti-Tuberculosis Association, Tokyo 204-8533, Japan[8]

Received 24 November 2007/Accepted 1 March 2008

***Mycobacterium avium-Mycobacterium intracellulare* complex (MAC) is the most common isolate of nontuberculous mycobacteria and causes pulmonary and extrapulmonary diseases. MAC species can be grouped into 31 serotypes by the epitopic oligosaccharide structure of the species-specific glycopeptidolipid (GPL) antigen. The GPL consists of a serotype-common fatty acyl peptide core with 3,4-di-*O*-methyl-rhamnose at the terminal alaninol and a 6-deoxy-talose at the *allo*-threonine and serotype-specific oligosaccharides extending from the 6-deoxy-talose. Although the complete structures of 15 serotype-specific GPLs have been defined, the serotype 16-specific GPL structure has not yet been elucidated. In this study, the chemical structure of the serotype 16 GPL derived from *M. intracellulare* was determined by using chromatography, mass spectrometry, and nuclear magnetic resonance analyses. The result indicates that the terminal carbohydrate epitope of the oligosaccharide is a novel *N*-acyl-dideoxy-hexose. By the combined linkage analysis, the oligosaccharide structure of serotype 16 GPL was determined to be 3-2′-methyl-3′-hydroxy-4′-methoxy-pentanoyl-amido-3,6-dideoxy-β-hexose-(1→3)-4-*O*-methyl-α-L-rhamnose-(1→3)-α-L-rhamnose-(1→3)-α-L-rhamnose-(1→2)-6-deoxy-α-L-talose. Next, the 22.9-kb serotype 16-specific gene cluster involved in the glycosylation of oligosaccharide was isolated and sequenced. The cluster contained 17 open reading frames (ORFs). Based on the similarity of the deduced amino acid sequences, it was assumed that the ORF functions include encoding three glycosyltransferases, an acyltransferase, an aminotransferase, and a methyltransferase. An *M. avium* serotype 1 strain was transformed with cosmid clone no. 253 containing *gtfB-drrC* of *M. intracellulare* serotype 16, and the transformant produced serotype 16 GPL. Together, the ORFs of this serotype 16-specific gene cluster are responsible for the biosynthesis of serotype 16 GPL.**

Mycobacterial diseases, such as tuberculosis and infection due to nontuberculous mycobacteria (NTM), are still among the most serious infectious diseases in the world. The incidence is increasing because of the spread of drug-resistant mycobacteria and the human immunodeficiency virus (HIV) infection/AIDS epidemic (16, 17, 30). *Mycobacterium avium-Mycobacterium intracellulare* complex (MAC) is the most common among isolates of NTM and is distributed ubiquitously in the environment. MAC causes pulmonary and extrapulmonary diseases in both immunocompromised and immunocompetent hosts. It affects primarily patients with advanced HIV infection. MAC includes at least two mycobacterial species, *M. avium* and *M. intracellulare*, that cannot be differentiated on the basis of traditional physical and biochemical tests (1, 41).

The cell envelope of mycobacteria is a complex and unusual structure. The key feature of this structure is an extraordinarily high lipid concentration (6, 10). To better understand the pathogenesis of MAC infection, it is necessary to elucidate the molecular structure and biochemical features of the lipid components. Among MAC lipids, the glycopeptidolipid (GPL) is of particular importance, because it shows not only serotype-specific antigenicity but also immunomodulatory activities in the host immune responses (2, 9, 23). Structurally, GPLs are composed of two parts, a tetrapeptide-amino alcohol core and a variable oligosaccharide (OSE). C_{26}-C_{34} fatty acyl-D-phenylalanine-D-*allo*-threonine-D-alanine-L-alaninol (D-Phe-D-*allo*-Thr-D-Ala-L-alaninol) is further linked with 6-deoxy talose (6-d-Tal) and 3,4-di-*O*-methyl rhamnose (3,4-di-*O*-Me-Rha) at D-*allo*-Thr and the terminal L-alaninol, respectively. This type of core GPL is found in all subspecies of MAC, shows a common antigenicity, and is further glycosylated at 6-d-Tal to form a serotype-specific OSE.

At present, 31 distinct serotype-specific GPLs have been identified serologically and chromatographically (9). Although the standard technique for differentiation of MAC subspecies

* Corresponding author. Mailing address: Department of Host Defense, Osaka City University Graduate School of Medicine, 1-4-3 Asahi-machi, Abeno-ku, Osaka 545-8585, Japan. Phone: 81 6 6645 3746. Fax: 81 6 6645 3747. E-mail: fujiwara@med.osaka-cu.ac.jp.

† Supplemental material for this article may be found at http://jb.asm.org/.

▽ Published ahead of print on 7 March 2008.

has been serotyping based on the OSE residue of its GPL, the complete structures of only 15 GPLs have been defined. In addition to the chemical structures of various GPLs, genes encoding the glycosylation pathways in the biosynthesis of GPL have been identified and characterized (12, 21, 31). Epidemiological studies have shown that MAC serotypes 4 and 8 are the most frequently isolated from patients, and MAC serotype 16 is one of the next most common groups (32, 40). It has been suggested that the serotypes of MAC isolates participate in their virulence (29), and thus, understanding of the structure-pathogenicity relationship of GPLs is necessary. In the present study, we demonstrate the complete OSE structure of the GPL derived from serotype 16 MAC (*M. intracellulare*), which has a unique terminal-acylated-amido sugar, and we characterized the serotype 16 GPL-specific gene cluster involved in the glycosylation of carbohydrates.

MATERIALS AND METHODS

Bacterial strains and preparation of GPL. *M. intracellulare* serotype 16 strain ATCC 13950^T (NF 115) was purchased from the American Type Culture Collection (Manassas, VA). Three clinical isolates of *M. intracellulare* serotype 16 (NF 116 and 117) and *M. avium* serotype 1 (NF 113) were maintained in The Research Institute of Tuberculosis, Japan Anti-Tuberculosis Association. The preparation of GPL was performed as described previously (18, 24, 26). Briefly, each strain of *M. intracellulare* serotype 16 was grown in Middlebrook 7H9 broth (Difco Laboratories, Detroit, MI) with 0.5% glycerol and 10% Middlebrook oleic acid-albumin-dextrose-catalase enrichment (Difco) at 37°C for 2 to 3 weeks. The heat-killed bacteria were sonicated, and crude lipids were extracted with chloroform-methanol (2:1, vol/vol). The extracted lipids were dried and hydrolyzed with 0.2 N sodium hydroxide in methanol at 37°C for 2 h. After neutralization with 6 N hydrochloric acid, alkaline-stable lipids were partitioned by a two-layer system of chloroform-methanol (2:1, vol/vol) and water. The organic phase was recovered, evaporated, and precipitated with acetone to remove any acetone-insoluble components containing phospholipids and glycolipids. The supernatant was collected by centrifugation, dried, and then treated with a Sep-Pak silica cartridge (Waters Corporation, Milford, MA) with washing (chloroform-methanol, 95:5, vol/vol) and elution (chloroform-methanol, 1:1, vol/vol) for partial purification. GPL was completely purified by preparative thin-layer chromatography (TLC) of Silica Gel G (20 by 20 cm, 250 μm; Uniplate; Analtech, Inc., Newark, DE). The TLC plate was repeatedly developed with chloroform-methanol-water (65:25:4 and 60:16:2, vol/vol/vol) until a single spot was obtained. After exposure of the TLC plate to iodine vapor, the GPL band was marked, and then, the silica gels were scraped off and the GPL was eluted with chloroform-methanol (2:1, vol/vol).

Preparation of OSE moiety. β elimination of GPL was performed with alkaline borohydride, and the OSE elongated from D-*allo*-Thr was released as described previously (18, 24). Briefly, the GPL was dissolved in ethanol, and an equal volume of 10 mg/ml sodium borohydride or borodeuteride in 0.5 N sodium hydroxide was added and then stirred at 60°C for 16 h. The reaction mixture was decationized with Dowex 50W-X8 beads (Dow Chemical Company, Midland, MI), collected, and evaporated under nitrogen to remove boric acid. The dried residue was partitioned in two layers of chloroform-methanol (2:1, vol/vol) and water. The upper aqueous phase was recovered and evaporated. In these processes, the serotype 16-specific OSE was purified as an oligoglycosyl alditol.

MALDI-TOF and MALDI-TOF/TOF MS analyses. The molecular species of the intact GPL was detected by matrix-assisted laser desorption ionization–time of flight mass spectrometry (MALDI-TOF MS) with an Ultraflex II (Bruker Daltonics, Billerica, MA). The GPL was dissolved in chloroform-methanol (2:1, vol/vol) at a concentration of 1 mg/ml, and 1 μl was applied directly to the sample plate, and then 1 μl of 10 mg/ml 2,5-dihydroxybenzoic acid in chloroform-methanol (1:1, vol/vol) was added as a matrix. The intact GPL was analyzed in the reflectron mode with an accelerating voltage operating in a positive mode of 20 kV (5). Then the fragment pattern of the OSE was analyzed with MALDI-TOF/TOF MS. The OSE was dissolved in ethanol-water (3:7, vol/vol), and the matrix was 10 mg/ml 2,5-dihydroxybenzoic acid in ethanol-water (3:7, vol/vol). The OSE and the matrix were applied to the sample plate according to the method for intact GPL and analyzed in the lift-lift mode.

GC and GC-MS analyses of carbohydrates and *N*-acylated short-chain fatty acid. To determine the glycosyl composition and linkage position, gas chromatography (GC) and GC-MS analyses of partially methylated alditol acetate derivatives were performed. Perdeuteromethylation was conducted by the modified procedure of Hakomori as described previously (18, 20). Briefly, the dried OSE was dissolved with a mixture of dimethyl sulfoxide and sodium hydroxide, and deuteromethyl iodide was added. The reaction mixture was stirred at room temperature for 15 min and then water and chloroform were added. The chloroform-containing perdeuteromethylated OSE layer was collected, washed with water two times, and then completely evaporated. Partially deuteromethylated alditol acetates were prepared from perdeuteromethylated OSE by hydrolysis with 2 N trifluoroacetic acid at 120°C for 2 h, reduction with 10 mg/ml sodium borodeuteride at 25°C for 2 h, and acetylation with acetic anhydride at 100°C for 1 h (8, 18, 25). To identify amino-linked fatty acids, acidic methanolysis of serotype 16 GPL was performed with 1.25 M hydrogen chloride in methanol (Sigma-Aldrich, St. Louis, MO) at 100°C for 90 min, and the fatty acid methyl esters were extracted with *n*-hexane under the cooled ice. GC was performed using a 5890 series II gas chromatograph (Hewlett Packard, Avondale, PA) equipped with a fused SPB-1 capillary column (30 m, 0.25-mm inner diameter; Supelco Inc., Bellefonte, PA). Helium was used for electron impact (EI)-MS and isobutane for chemical ionization (CI)-MS as a carrier gas. A JMS SX102A double-focusing mass spectrometer (JEOL, Tokyo, Japan) was connected to the gas chromatograph as a mass detector. The molecular separator and the ion source energy were 70 eV for EI and 30 eV for CI, and the accelerating voltage was 8 kV. The D and L configurations of Rha residues were determined by comparative GC-MS analysis of trimethylsilylated (*S*)-(+)-sec-butyl glycosides and (*R*)-(−)-sec-butyl glycosides prepared from an authentic standard L-Rha (19).

NMR analysis of GPL. The GPL was dissolved in chloroform-d ($CDCl_3$)-methanol-d_4 (CD_3OD) (2:1, vol/vol). To define the anomeric configurations of each glycosyl residue, ^1H and ^{13}C nuclear magnetic resonance (NMR) was employed. Both homonuclear correlation spectrometry (COSY) and ^1H-detected [^1H, ^{13}C] heteronuclear multiple-quantum correlation (HMQC) were recorded with a Bruker Avance-600 (Bruker BioSpin Corp., Billerica, MA), as described previously (9, 18, 24, 34).

Construction of *M. intracellulare* serotype 16 cosmid library. A cosmid library of *M. intracellulare* serotype 16 strain ATCC 13950^T was constructed as described previously (18). Bacterial cells were disrupted mechanically, and genomic DNA was extracted with phenol-chloroform and then precipitated with ethanol. Genomic DNA randomly sheared into 30- to 50-kb fragments in the extraction process was fractionated and electroeluted from agarose gels using a Takara Recochip (Takara, Kyoto, Japan). These DNA fragments were rendered blunt ended using T4 DNA polymerase and deoxynucleoside triphosphates and then were ligated to dephosphorylated arms of pYUB412 (XbaI-EcoRV and EcoRV-XbaI), which were the kind gifts of William R. Jacobs, Jr. (Department of Microbiology and Immunology, Albert Einstein College of Medicine, Bronx, NY). The cosmid vector pYUB412 is an *Escherichia coli-Mycobacterium* shuttle vector with the *int-attP* sequence for integration into a mycobacterial chromosome, *oriE* for replication in *E. coli*, a hygromycin resistance gene, and an ampicillin resistance gene. After in vitro packaging using Gigapack III Gold extracts (Stratagene, La Jolla, CA), recombinant cosmids were introduced into *E. coli* STBL2 [F$^-$ *mcrA* Δ(*mcrBC-hsdRMS-mrr*) *recA1 endA1 lon gyrA96 thi supE44 relA1* λ Δ(*lac-proAB*)] and stored at −80°C in 50% glycerol.

Isolation of cosmid clones carrying biosynthesis gene cluster of serotype 16 GPL and sequence analysis. Isolation of DNA from *E. coli* transductants was performed as described by Supply et al., with modifications (39). The colonies were picked, transferred to a 1.5-ml tube containing 50 μl of water, and then heated at 98°C for 5 min. After centrifugation at 14,000 rpm for 5 min, the supernatant was used as the PCR template. PCR was used to isolate cosmid clones carrying the rhamnosyltransferase (*rtfA*) gene with primers rtfA-F (5′-TTTGGAGCGACGAGTTCATC-3′) and rtfA-R (5′-GTGTAGTTGACCACG CCGAC-3′). *rtfA* encodes an enzyme responsible for the transfer of Rha to 6-d-Tal in OSE (14, 31). The insert of cosmid clone no. 253 was sequenced using a BigDye Terminator, version 3.1, cycle sequencing kit (Applied Biosystems, Foster City, CA) and an ABI Prism 310 gene analyzer (Applied Biosystems). The putative function of each open reading frame (ORF) was identified by similarity searches between the deduced amino acid sequences and known proteins using BLAST (http://www.ncbi.nlm.nih.gov/BLAST/) and FramePlot (http://www.nih.go.jp/~jun/cgi-bin/frameplot.pl) with the DNASIS computer program (Hitachi Software Engineering, Yokohama, Japan).

Transformation of *M. avium* serotype 1 strain with cosmid clone no. 253. An *M. avium* serotype 1 strain (NF113) was transformed with pYUB412-cosmid clone no. 253 by electroporation, and hygromycin-resistant colonies were iso-

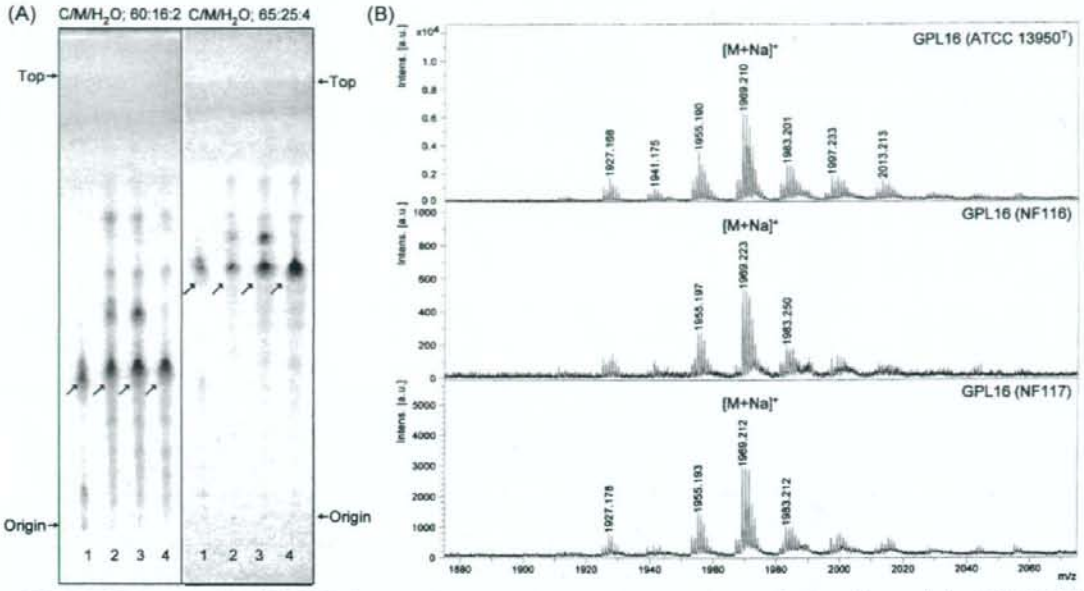

FIG. 1. TLC patterns and MALDI-TOF MS spectra of serotype 16 GPL. (A) Serotype 16 GPL purified from *M. intracellulare* ATCC 13950^T (NF 115) and the alkaline-stable lipids derived from ATCC 13950^T and two clinical isolates (NF 116 and 117) from left to right were developed on TLC plates with solvent systems of chloroform-methanol-water (65:25:4 and 60:16:2, vol/vol/vol). (B) The MALDI-TOF MS spectra were acquired using 10 mg/ml 2,5-dihydroxybenzoic acid in chloroform-methanol (1:1, vol/vol) as a matrix, and the molecularly related ions were detected as $[M+Na]^+$ in positive mode. Intens., intensity; a.u., absorbance units.

lated. Alkaline-stable lipids were prepared, and productive GPLs were examined by TLC and MALDI-TOF MS analyses.

Nucleotide sequence accession number. The nucleotide sequence reported here has been deposited in the NCBI GenBank database under accession no. AB355138.

RESULTS

Purification and molecular weight of intact GPL. Serotype 16 GPL from *M. intracellulare* ATCC 13950^T (NF 115) was detected as a spot by TLC, and the R_f values were 0.35 and 0.56 when developed with chloroform-methanol-water (60:16:2 and 65:25:4, vol/vol/vol, respectively). Two clinical isolates of *M. intracellulare*, NF 116 and 117, had serotype 16 GPLs that showed the same R_f values as the serotype 16 GPL derived from strain ATCC 13950^T. The serotype 16 GPL of *M. intracellulare* strain ATCC 13950^T was purified repeatedly by TLC and was shown as a single spot by TLC (Fig. 1A). The MALDI-TOF MS spectra of each serotype 16 GPL showed *m/z* 1969 for $[M+Na]^+$ as the main molecularly related ion in positive mode, with the homologous ions differing by 14 mass units at 1,955 and 1,983 (Fig. 1B). As a result, the main molecular weight of serotype 16 GPL was 1,946, which implied that it has a novel carbohydrate chain elongated from D-*allo*-Thr.

Carbohydrate composition of serotype 16 OSE. To determine the glycosyl compositions of serotype 16 OSE, alditol acetate derivatives of the serotype 16 GPL were analyzed by GC and GC-MS. The structurally defined serotype 4 GPL was used as a reference standard (9, 35). Comparison of the retention time and GC mass spectra (Fig. 2) with the alditol acetate derivatives of the serotype 16 GPL showed the presence of 3,4-di-*O*-Me-Rha, 4-*O*-Me-Rha, Rha, 6-d-Tal, and an unknown sugar residue (X1) in a ratio of approximately 1:1:2:1:1. The alditol acetate of X1 was eluted at a retention time of 29.3 min, greater than that of glucitol acetate on the SPB-1 column. The CI-MS spectrum of X1 was $[M+H]^+$ at *m/z* 520 as a parent ion and *m/z* 460 as a loss of 60 (acetate). The fragment ions of X1 sugar showed characteristic patterns in EI-MS. *m/z* 360 indicated the cleavage of C-3 and C-4, and *m/z* 300, 240, and 180 were fragmented with a loss of 60 (acetate). Similarly, *m/z* 374 indicated the cleavage of C-2 and C-3, and *m/z* 314 and 254 were fragmented with a loss of 60 (Fig. 3A and B). These results indicated that X1 was 3,6-dideoxy hexose (Hex). The odd molecular weight of X1, 519, and *m/z* 187, 127, and 59 implied the presence of one amido group esterified with a short-chain fatty acid, possibly. After methanolysis of serotype 16 GPL, the resultant fatty acid methyl esters were extracted carefully and analyzed by GC-MS. The EI-MS spectrum of a short-chain fatty acid methyl ester showed mass ions at *m/z* 176 ($[M]^+$), 145 ($[M-31]^+$), 117 ($[M-59]^+$), 99, 88, 85, and 59 (Fig. 3C) (33, 37). Taking the results together, X1 was structurally determined to be 3-2′-methyl-3′-hydroxy-4′-methoxy-pentanoyl-amido-3,6-dideoxy-Hex.

Glycosyl linkage and sequence of serotype 16 OSE. To determine the glycosyl linkage and sequence of the OSE, GC-MS of perdeuteromethylated alditol acetates and MALDI-TOF/TOF MS of the oligoglycosyl alditol from serotype 16 OSE

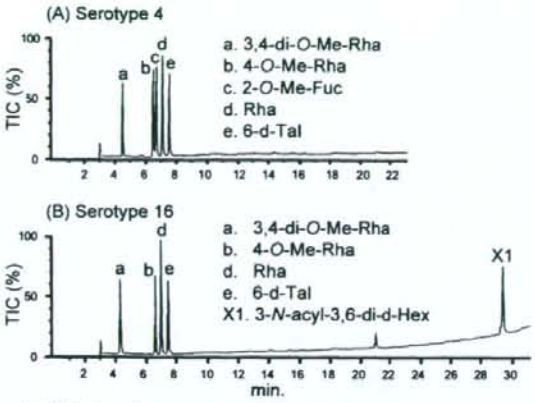

FIG. 2. Gas chromatograms of the alditol acetate derivatives from serotype 4 (A) and serotype 16 (B) GPLs. Total ion chromatograms (TIC) are shown. GC was performed on an SPB-1-fused silica column with a temperature program of 160°C for 2 min, followed by an increase of 4°C/min to 220°C, and holding at 220°C for 15 min. Comparison to the GC spectrum of serotype 4 GPL shows that serotype 16 GPL is composed of 3,4-di-*O*-Me-Rha, 4-*O*-Me-Rha, Rha, 6-d-Tal, and an unknown X1 sugar residue.

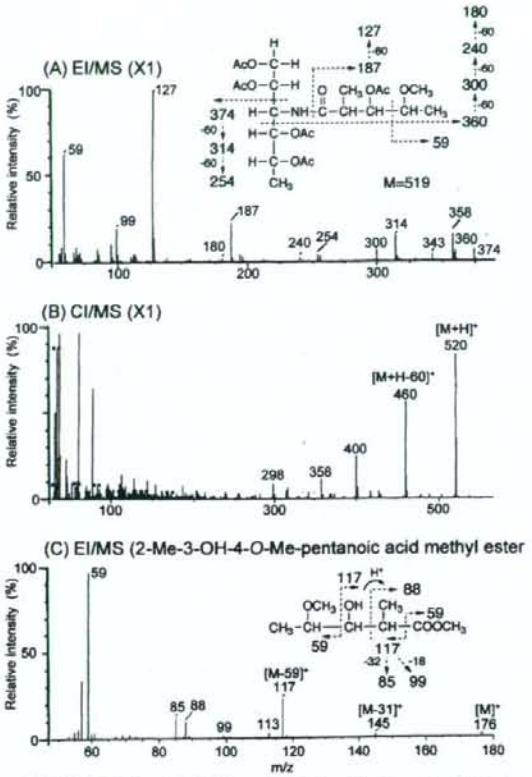

FIG. 3. EI-MS and CI-MS spectra of the alditol acetate derivative from X1 (A and B) and *N*-acylated-short-chain fatty acid methyl ester (C). The pattern of prominent fragment ions is illustrated. The CG column and condition were described in the legend for Fig. 2.

were performed. As shown in Fig. 4, the GC-MS spectra of perdeuteromethylated alditol acetates were assigned four major peaks, 1,3,4,5-tetra-*O*-deuteromethyl-2-*O*-acetyl-6-deoxytalitol (*m/z* 109, 132, 154, 167, and 214); 2,4-di-*O*-deuteromethyl-1,3,5-tri-*O*-acetyl-rhamnitol (*m/z* 121, 134, 205, 240, and 253); 2-*O*-deuteromethyl-4-*O*-methyl-1,3,5-tri-*O*-acetyl-rhamnitol (*m/z* 121, 131, 202, and 237); and 2,4-di-*O*-deuteromethyl-1,5-di-*O*-acetyl-3-2′-methyl-3′-*O*-deuteromethyl-4′methoxypentanoyl-deuteromethylamido-3,6-dideoxy-hexitol (*m/z* 121, 134, and 341). These results revealed that the 6-d-Tal residue was linked at C-2; Rha and 4-*O*-Me-Rha were linked at C-1 and C-3; and the nonreducing terminus, 3-2′-methyl-3′-hydroxy-4′-methoxy-pentanoyl-amido-3,6-dideoxy-Hex, was C-1 linked. The MALDI-TOF/TOF MS spectrum of the oligoglycosyl alditol from serotype 16 OSE afforded the expected molecular ions $[M+Na]^+$ at *m/z* 931, together with the characteristic mass increments in the series of glycosyloxonium ions formed on fragmentation at *m/z* 312, 472, 618, and 764 from the terminal sugar *N*-acyl-Hex to 6-d-Tal and at *m/z* 336, 482, and 642 from 6-d-Tal to *N*-acyl-Hex (Fig. 5). Rha residues were determined to be in the L absolute configuration by comparative GC-MS analyses of trimethylsilylated (*S*)-(+)-sec-butyl glycosides and (*R*)-(−)-sec-butylglycosides (see Fig. S1 in the supplemental material). Taken together, these results established the sequence and linkage arrangement 3-2′-methyl-3′-hydroxy-4′-methoxy-pentanoyl-amido-3,6-dideoxy-Hex-(1→3)-4-*O*-Me-Rha-(1→3)-L-Rha-(1→3)-L-Rha-(1→2)-6-d-Tal, exclusively.

NMR analysis of serotype 16 OSE. The ^{1}H NMR and ^{1}H-^{1}H COSY analyses of the serotype 16 GPL revealed six distinct anomeric protons with corresponding H1-H2 cross peaks in the low field region at δ4.93, 4.92, 4.92, 4.84, 4.65 ($J_{1\text{-}2}$ = 2 to 3 Hz, indicative of α-anomers) and 4.51 (a doublet, $J_{1\text{-}2}$ = 7.7 Hz, indicative of a β-hexosyl unit). When further analyzed by ^{1}H-detected [^{1}H, ^{13}C] two-dimensional HMQC, the anomeric protons resonating at δ4.93, 4.92, 4.92, 4.84, 4.65, and 4.51 have C-1s resonating at δ101.57, 95.73, 101.40, 102.56, 100.97, and 103.36, respectively (for a summary, see Table S1 in the supplemental material). The J_{CH} values for each of these protons were calculated to be 171, 170, 171, 170, 169, and 161 Hz by measurement of the inverse-detection nondecoupled two-dimensional HMQC (Fig. 6). These results established that the terminal amido-Hex was a β configuration and the others were α-anomers.

Cloning and sequence of serotype 16 GPL biosynthesis cluster. To isolate the serotype 16 GPL biosynthesis cluster, the genomic cosmid library of *M. intracellulare* serotype 16 strain ATCC 13950^T was constructed. Primers were designed to amplify the region corresponding to the *rtfA* gene. More than 300 cosmid clones were tested using colony PCR with *rtfA* primers, and the positive clones no. 51 and 253 were isolated from the *E. coli* transductants. PCR analysis revealed that clone no. 253 contained a *drrC* gene but that clone no. 51 did not. Thus, we used clone no. 253 for subsequent sequence analysis for the *gtfB-drrC* region. The 22.9-kb region of *M. intracellulare* sero-

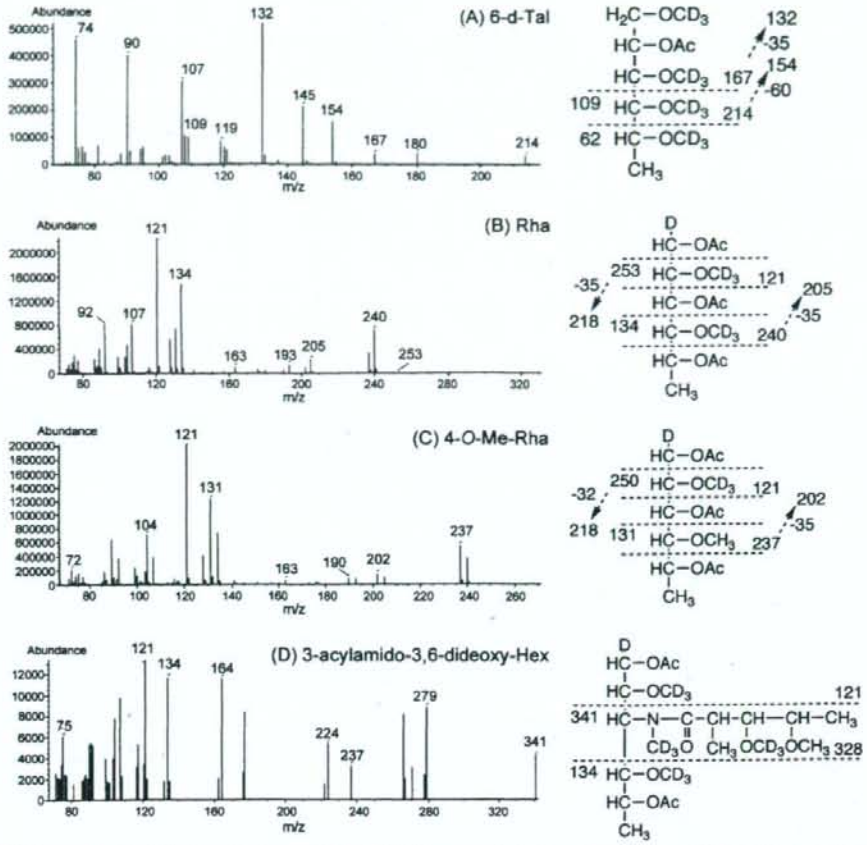

FIG. 4. GC-MS spectra of individual perdeuteromethylated alditol acetate derivatives from serotype 16 OSE. The formation of prominent fragment ions is illustrated; fragments were assigned to 1,3,4,5-tetra-*O*-deuteromethyl-2-*O*-acetyl-6-deoxy-talitol (A), 2,4-di-*O*-deuteromethyl-1,3,5-tri-*O*-acetyl-rhamnitol (B), 2-*O*-deuteromethyl-4-*O*-methyl-1,3,5-tri-*O*-acetyl-rhamnitol (C), and 2,4-di-*O*-deuteromethyl-1,5-di-*O*-acetyl-3-2′-methyl-3′-*O*-deuteromethyl-4′-methoxy-pentanoyl-deuteromethylamido-3,6-dideoxy-hexitol (D).

type 16 ATCC 13950^T was deposited in the NCBI GenBank database (accession no. AB355138). The similarity to protein sequences of each ORF is summarized in Table 1, and the genetic map for the serotype 16 GPL biosynthetic cluster was compared with those of serotype 2, 4, and 7 GPLs (Fig. 7). The *gtfB* and *drrC* genes of *M. intracellulare* serotype 16 ATCC 13950^T had 99.8% and 83.7% DNA identities with those of *M. intracellulare* serotype 7 ATCC 35847, respectively. In the DNA region between *gtfB* and *drrC* (20.8 kb), 17 ORFs were observed. Four ORFs (ORF 1, 2, 16, and 17) were homologous to those found in the same region of serotype 7-specific DNA, and the others were unique to the serotype 16 strain. No insertion of insertion elements or transposons was detected in this region. The nucleotide sequences of the ORF 1 and ORF 2 in serotype 16 strain ATCC 13950^T were homologous to those of ORF 1 and ORF 8 in serotype 7, respectively, suggesting that these two ORFs have the same function. The similarity of the deduced amino acid sequences suggested the possibility that the functions of ORF 3 and ORF 6 are to encode methyltransferase and aminotransferase, respectively. The deduced amino acid sequences of ORF 4 and ORF 5 showed significant similarities to the WxcM protein, the function of which is not clear. Interestingly, the deduced amino acid sequences of ORF 16 and ORF 17 of serotype 16 were homologous to ORF 9 of serotype 7. ORFs 1, 16, and 17 have considerable homology to glycosyltransferases. Nine ORFs, which are possibly involved in fatty acid synthesis, were detected between ORF 7 and ORF 15. It is notable that ORF 13 had a chimeric structure. The N-terminal half of ORF 13 showed similarity to phosphate butyryl/acetyl transferases, but the C-terminal half showed similarity to short-chain reductase/dehydrogenases. These results suggest that this region of DNA is responsible for the biosynthesis of the serotype 16-specific GPL.

Expression of cosmid clone no. 253 in *M. avium* serotype 1 strain. The OSE of serotype 1 GPL was composed of α-L-Rha-